Under phosphate starvation conditions, Fe and Al trigger accumulation of the transcription factor STOP1 in the nucleus of Arabidopsis root cells

Christian Godon, Caroline Mercier, Xiaoyue Wang, Pascale David, Pierre Richaud, Laurent Nussaume, Dong Liu, Thierry Desnos

the plant journal

Under phosphate starvation condition, Fe and Al trigger the transcription factor STOP1 to accumulate in the nucleus of Arabidopsis root cells.

Journal:	*The Plant Journal*
Manuscript ID	TPJ-01389-2018.R1
Manuscript Type:	Original Article
Key Words:	phosphate, iron, aluminum, root, STOP1, ALMT1, Arabidopsis, ALS3

Running head
Fe and Al trigger nuclear accumulation of STOP1

Under phosphate starvation condition, Fe and Al trigger the transcription factor STOP1 to accumulate in the nucleus of Arabidopsis root cells

Christian Godon[1]*, Caroline Mercier[1]*, Xiaoyue Wang[2], Pascale David[1], Pierre Richaud[3], Laurent Nussaume[1], Dong Liu[2,4], Thierry Desnos[1,4]

[1] Laboratoire de Biologie du Développement des Plantes, Commissariat à l'Energie Atomique et aux énergies alternatives, UMR7265 (CEA, Aix-Marseille Université, CNRS), Saint Paul-Lez-Durance F-13108, France.

[2] Ministry of Education Key Laboratory of Bioinformatics, Center for Plant Biology, School of Life Sciences, Tsinghua University, Beijing 100084, China

[3] Laboratoire de Bioénergétique et Biotechnologie des Bactéries et Microalgues, Commissariat à l'Energie Atomique et aux énergies alternatives, UMR7265 (CEA, Aix-Marseille Université, CNRS), Saint Paul-Lez-Durance F-13108, France.

* These authors contributed equally to this work.
[4] Authors for correspondence.

Abstract

Low-phosphate (Pi) condition is known to repress the primary root growth of Arabidopsis, in a low-pH and Fe-dependent manner. This growth arrest requires the accumulation of STOP1 transcription factor in the nucleus where it activates the transcription of the malate transporter gene *ALMT1*; exuded malate is suspected to interact with extracellular iron to inhibit root growth. In addition, ALS3 –an ABC-like transporter first identified for its role for tolerance to toxic aluminum– represses nuclear accumulation of STOP1 and the expression of *ALMT1*.
Until now, it was unclear whether phosphate deficiency itself or iron activates STOP1 to accumulate in the nucleus.
Here, by using different growth media to dissociate the effects of Fe from Pi deficiency itself, we demonstrate that Fe is sufficient to trigger the accumulation of STOP1 in the nucleus, which in turn, activates the expression of *ALMT1*. We also show that a low pH is necessary to stimulate the Fe-dependent accumulation of nuclear STOP1. Furthermore, pharmacological experiments indicate that Fe inhibits proteasomal degradation of STOP1. We also show that Al acts like Fe for nuclear STOP1 accumulation and *ALMT1* expression, and that the overaccumulation of STOP1 in the nucleus of the *als3* mutant grown in low-Pi could be abolished by Fe deficiency. Altogether, our results indicate that, under low-Pi condition, $Fe^{2/3+}$ and Al^{3+} act similarly to increase the stability of STOP1 and its accumulation in the nucleus where it activates the expression of *ALMT1*.

Significance Statement

Low-phosphate, low-pH and excess aluminum are three major stresses inhibiting root growth. The Arabidopsis transcription factor STOP1 has a major role in root growth

under these different stresses, but how STOP1 is regulated is not known. Here we show that Fe –instead of low-phosphate– and Al promote the accumulation of STOP1 in root nuclei, in a low-pH-dependent manner. This work unveils an important regulatory step in the response to Al and Fe stresses.

Keywords
STOP1, ALMT1, ALS3, phosphate, iron, aluminum, pH, root, nucleus, Arabidopsis.

Introduction

In many plant species, Pi-deficiency (-Pi) alters root growth and architecture promoting top-soil foraging: the growth of the primary root is reduced whereas lateral root emergence and growth is stimulated toward a more horizontal direction. Combined, these responses result in root systems that explore relatively better the upper soil horizons where Pi is more concentrated (Lynch, 2001).

The Arabidopsis primary root stops growing when its apex encounters the -Pi substratum (Svistoonoff et al., 2007). Split-root and feeding experiments showed that this root grow inhibition does not correlate with Pi accumulated inside the root (Thibaud et al., 2010). Instead, it depends of the Pi concentration in the growth medium. This phenomenon was described as the so-called –Pi local response, by opposition to the -Pi systemic responses that are governed by Pi concentration present inside the plant tissues (Puga et al., 2017). While the -Pi systemic response is mainly controlled by the two master regulatory genes *PHOSPHATE STARVATION RESPONSE 1* (*PHR1*) and *PHR1-like 1* (*PHL1*), the -Pi local response is not (Balzergue et al., 2017). This local growth inhibition response critically depends of the Fe-content of the growth medium (Svistoonoff et al., 2007, Ward et al., 2008, Muller et al., 2015), and iron accumulates in the root tip (Muller et al., 2015, Balzergue et al., 2017, Mora-Macias et al., 2017).

Inherent to its chemical properties, Pi can form complexes with metallic cations such as $Fe^{2/3+}$ and Al^{3+} (Hinsinger, 2001). This has important consequences for the mobility and bioavailability in soil of Pi, Fe and Al as well as for their homeostasis in plants (Hirsch et al., 2006, Misson et al., 2005, Briat et al., 2015, Bouain et al., 2014). In the medium, reflecting the antagonistic Fe-Pi interactions, the Pi/Fe ratio is important: the lower the ratio the higher the inhibition, and when the nutrient solution lacks Fe, the root growth is no more inhibited (Ward et al., 2008, Muller et al., 2015, Svistoonoff et al., 2007).

During the last decade, major advances contributed to a better understanding of the cellular events underlying the “local” response in Arabidopsis. When exposed to low external Pi (i.e. a low Pi/Fe ratio), the short primary root results from a combination of rapid as well as long-term cellular responses at the root tip. Few hours, if not minutes, after the root tip encounters a Pi-depleted zone, cell elongation decreases. This is correlated with the deposition of iron and accumulation of reactive oxygen species (ROS) in the cell wall of the stem cell niche (SCN) and the elongation zone (EZ), and with a peroxidase-dependent stiffening of the cell wall of the EZ.

In the long term (hours to days), callose accumulates in cell wall of the root apical meristem (RAM) and EZ, this occludes plasmodesmata and restricts cell-to-cell trafficking. Progressively, root cell proliferation ceases until the exhaustion of the RAM by the on-going cell differentiation (Balzergue et al., 2017, Muller et al., 2015, Mora-Macias et al., 2017).

Genetics and molecular analysis identified several proteins governing the root growth inhibition under -Pi. Identified as a major quantitative trait locus, LOW PHOSPHATE ROOT 1 (LPR1) codes a cell wall multicopper oxidase with ferroxidase activity (Svistoonoff et al., 2007, Ticconi et al., 2009, Muller et al., 2015, Reymond et al., 2006). LPR1 has a critical role in the growth arrest because loss-of-function mutations in *lpr1* desensitize the root to -Pi. In particular, they accumulate reduced amount of Fe in their root tip. Upon extended Pi-deprivation, the LPR1-dependent Fe accumulation promotes RAM exhaustion and differentiation by the down-regulation of the root patterning transcription factors SHORT ROOT (SHR) and SCARECROW (SCR). This regulation operates via increased expression of CLAVATA 4 (CLV4), a secreted peptide detected by the plasma membrane receptors CLV2 and CLV2/PEP1 RECEPTOR 2 (PEPR2) (Gutiérrez-Alanís et al., 2017). A higher level of regulation coupling LPR1 with brassinosteroid (BR) signalling pathways has been recently unveiled. In particular, the root growth of seedlings with the constitutively active *bzr1-D* mutation (*BZR1* for *BRASSINAZOLE RESISTANT1*) are unrepressed in -Pi and has reduced expression of *LPR1* (Singh et al., 2014, Singh et al., 2018). In addition, in the wild type (WT), Fe enhances the accumulation of the BR-signalling inhibitor BKI1 (BRASSINSOSTEROID KINASE INHIBITOR1), thereby closing a feedback regulatory loop between LPR1 activity and BR signalling.

PHOSPHATE DEFICIENCY RESPONSE 2 (*PDR2*) was the first gene identified in the local response (Ticconi et al., 2004). PDR2 is the only Arabidopsis P5-type ATPase; it is located in the endoplasmic reticulum and its substrate is not yet known (Ticconi et al., 2009). Compared to *lpr1* mutations, a mutation inactivating *PDR2* confers an opposite effect (i.e. over accumulation of Fe) (Muller et al., 2015). The *lpr1* mutations are epistatic over *pdr2* indicating a functional interaction between LPR1 and PDR2.

A large-scale forward genetics screen for seedlings with a primary root less sensitive to -Pi inhibition identified several *stop1* and *almt1* mutants (in addition to *lpr1*) (Balzergue et al., 2017). STOP1 (SENSITIVE TO PROTON RHIZOTOXICITY1) is a C_2H_2 zinc finger transcription factor necessary for the expression of *ALUMINUM ACTIVATED MALATE TRANSPORTER 1* (*ALMT1*), coding a plasma membrane transporter exuding malate (Hoekenga et al., 2006, Iuchi et al., 2007). While the *stop1* and *almt1* mutants have reduced accumulation of Fe in the EZ, they still accumulate large amount of Fe in the stem cell niche (SCN) (Balzergue et al., 2017, Wang et al., 2019), although others observed reduced accumulation of Fe in SCN (Mora-Macias et al., 2017). This is correlated with some remaining root inhibition upon long-term -Pi deprivation, presumably mediated by the Fe-dependent RAM differentiation and exhaustion. These observations show that the STOP1-ALMT1 module is mainly involved in the inhibition of cell elongation whereas the LPR1-PDR2 module influences all aspects of the local response. Supporting independent genetic regulations of these two modules, the *lpr1* mutation does not alter the expression of *ALMT1* and, reciprocally, *stop1* mutants display WT expression of *LPR1*. It seems that, at least in the elongation zone, the convergence point of these two modules is in the apoplast compartment where the ALMT1-exuded malate somehow helps the Fe to participate in the generation of ROS.

In the root tip, Pi deprivation enhances the transcript level of *ALMT1* but not of *STOP1*, suggesting a post-translational regulation of STOP1 protein. Indeed, the -Pi condition stimulates the accumulation of STOP1 in the nucleus (Balzergue et al.,

2017). This nuclear accumulation of STOP1 represents therefore an important control step in this pathway for which a first, and unexpected, regulatory component has been identified recently. A genetics screen for mutants hypersensitive to -Pi-induced root growth inhibition retrieved an *als3* mutant. The ALS3 protein (ALUMINUM SENSITIVE 3) interacts with STAR1 (SENSITIVE TO ALUMINUM RHIZOTOXICITY 1) to form a putative ATP-binding cassette (ABC) transporter complex located in the tonoplast (Dong et al., 2017). Consistently, in -Pi, the *star1* mutant behaves like *als3*. Interestingly, the root hypersensitivity of *als3* and *star1* correlates with higher accumulation of STOP1 in root nuclei and overexpression of *ALMT1* in the root tip. By contrast, in -Pi, the overexpression of the ALS3-STAR1 fusion protein represses the accumulation of STOP1 in the nucleus and improves root growth of WT. Moreover, a suppressor screen of *als3* identified *stop1* and *almt1* mutants (as well as *lpr1*) (Wang et al., 2019). Taken together, these results show that, in combination, ALS3 and STAR1 attenuate the root growth inhibition in -Pi by repressing the accumulation of STOP1 in the nucleus. This led us to hypothesize that ALS3-STAR1 depletes an unknown cytosolic compound (toward the vacuole) that enhances the accumulation of STOP1 in the nucleus (Wang et al., 2019).

Before the discovery of their implication in the response to -Pi, STOP1, ALMT1, ALS3 and STAR1 were all known for their major role in Arabidopsis resistance against toxic aluminum. Loss-of-function mutations in any of these genes severely impair root growth in the presence of Al^{3+} (Larsen et al., 2005, Iuchi et al., 2007, Huang et al., 2010, Hoekenga et al., 2006). It is therefore tempting to deduce that in Pi deprived conditions, $Fe^{2/3+}$ is the responsible metallic ion triggering nuclear accumulation of STOP1, thereby participating to root growth repression in -Pi.

In this work, we found growth conditions with limited Pi allowing to distinguish the effect of Fe from the -Pi *per se*. This enabled us to compare the effect of Fe with Al on STOP1 and ALMT1. Our results demonstrate that Fe, as well as Al, triggers the accumulation of STOP1 in the nucleus and the expression of *ALMT1*.

Results

We previously showed that the low-Pi condition stimulates the expression of the *ALMT1* gene, and this stimulation relies of the transcription factor STOP1 (Balzergue et al., 2017). In addition, under low-Pi, omitting Fe in the nutrient solution prevents the root growth arrest, showing that Fe is essential for this growth response (Svistoonoff et al., 2007, Ward et al., 2008, Dong et al., 2017, Muller et al., 2015, Mora-Macias et al., 2017). However, the -Fe conditions previously tested did not completely supressed the expression of *ALMT1*.

Fe, but not Pi deficiency *per se*, induces *ALMT1* expression

We used the *pALMT1::GUS* (GUS, β-glucuronidase) construct to investigate the role of Fe because this visual reporter sensitively allows to test the activity of the STOP1 signalling in the root tip (Balzergue et al. 2017). We first tested the influence of the Pi/Fe ratio on the expression of *ALMT1*. Seedlings were first grown 3 days on a -Pi medium without Fe added. To prevent the expression of *ALMT1* (and thus the accumulation of the GUS protein) during this pre-culture, the growth medium was buffered at pH 6.7. Indeed, at pH around neutrality we observed no or very little GUS staining in the root tip of *pALMT1::GUS* seedlings (Balzergue et al. 2017 & Figure S1). Seedlings were then transferred from this pre-culture condition, to media

differing by their Fe to Pi ratio, at pH 5.5. Twenty-four hours after transfer, the seedlings were stained for GUS activity. In a medium supplemented with 15 μM of Fe, and without Pi added, there is a strong expression of *ALMT1* (Figure 1a). Increasing the Pi content reduces the expression of *ALMT1*. However, at the highest Pi concentration tested (250 μM), the expression of *ALMT1* is still induced. This result confirms that *ALMT1* expression is higher in -Pi compared to +Pi condition. However, increasing the Fe content in a medium containing 250 μM Pi, increases the expression of *ALMT1* (Figure 1b). This confirms result of Müller et al (2015) and suggests that Fe, instead of Pi deficiency *per se*, stimulates the expression of *ALMT1*.

We observed that even without supplementing the -Pi growth medium with Fe, at pH 5.5, there was still a strong expression of *ALMT1* (Figure 2a, first picture). It prompted us to assay putative presence of iron in the agar using a quantification by ICP-AES (Inductively Coupled Plasma – Absorption Emission Spectrometry). This analysis revealed the presence of 38 μg $Fe.g^{-1}$ agar (5.5 μM Fe in the final growth medium) (Table S1).

To further test the hypothesis that, in -Pi condition, the Fe that was contained in the agar powder is the trigger of *ALMT1* expression, we reduced the availability of Fe in the growth media using a siderophore. Supplementing the medium with 100 μM deferoxamine (DFO), a potent Fe-chelator, strongly diminished *ALMT1* expression, (Figure 2a). DFO was effective in chelating Fe since addition of 15 μM Fe did not stimulate expression of *ALMT1* (Figure 2a). To avoid the potential toxicity of a high concentration of DFO that could interfere with gene expression, an alternative approach was used to reduce bioavailable iron from the agar. The agar powder was mixed with DFO and then washed (see Experimental procedures). We then tested whether the level of expression of *ALMT1* remained low. In -Pi plates made with this washed, DFO-treated agar, the expression of *ALMT1* is almost fully abolished, and addition of 15 μM Fe restored a high level of expression (Figure 2b). We conclude that a strong chelator of Fe suppresses the expression of *ALMT1*. Altogether, these results show that the stimulation of *ALMT1* expression in -Pi condition is triggered by Fe but not by the Pi-deficiency *per se*.

This result prompted us to compare the expression of *ALMT1* with that of *SPX1* (SYG1/Pho81/XPR1), a classical marker of the -Pi stress. *SPX1* encodes a protein regulating the activity of the transcription factor PHR1 –a master regulator of the -Pi stress, and is frequently used as a marker of the -Pi transcriptional response. To monitor its expression, we used WT seedlings containing the *pSPX1::GUS* marker (Duan et al., 2008). The *pALMT1::GUS* and *pSPX1::GUS* seedlings were grown in + or -Pi, at pH 5.5 or 6.7, and with two different agars or an agarose; in all these media the nutrient solution was not supplemented with Fe.

As already shown (Balzergue et al., 2017), on an agar containing Fe, the expression of *ALMT1* is induced at pH 5.5 but not at pH 6.7, in both -Pi and +Pi (Figure 3a). This expression is much less stimulated in media that contain very low amount of Fe (DFO-treated agar or on the agarose Seakem, Figure 3a and Supplementary Table 1). By contrast, the expression of *SPX1* is induced only in -Pi conditions, whatever the pH or the gelifying agent used to prepare the growth medium (Figure 3a). All these observations were confirmed by qRT-PCR (Quantitative Reverse Transcriptase-Polymerase Chain Reaction) (Figure 3b and Figure S2), and with the *PPsPase1* (pyrophosphatase [PPi]-specific phosphatase1) gene as an additional

marker whose expression is highly stimulated by Pi-deficiency (Hanchi et al., 2018) (Figure 3b).
We also monitored the expression of the *IRT1* (IRON-REGULATED TRANSPORTER 1) gene, a well-known indicator of Fe deficiency (Vert et al., 2002). This marker indicates that, as expected, when grown on the Sigma-DFO agar plates, seedlings are more Fe starved than on the other plates (Figure 3b). On plates made with the Seakem agar, that contains very low amount of Fe, *IRT1* is also more expressed than with the Sigma agar (Figure 3b). These analyses of genes expression further show that *ALMT1* is not stimulated by the -Pi *per se*, and strongly suggest that the signal stimulating the expression of *ALMT1* is distinct from that of the SPX1 pathway. By contrast to *ALMT1* mRNA, Al, Fe and pH do not modulate the level of *STOP1* mRNA accumulation (Figure S3).

Fe stimulates STOP1 accumulation in the nucleus

With the *pSTOP1::GFP-STOP1* reporter, we previously showed that STOP1 accumulates in the nuclei at the primary root tip seedlings grown in -Pi (Balzergue et al., 2017, Wang et al., 2019). Our gene expression analysis of *ALMT1* incited us to test whether Fe is involved in this nuclear accumulation of STOP1.
Seedlings carrying the *pSTOP1::GFP-STOP1* marker were grown 3 days in non-inducible conditions (i.e. agarose Seakem without addition of Pi and Fe that do not stimulate the expression of *ALMT1*, as shown in Figure 3a), transferred in the same medium supplemented or not with Fe before examining the GFP-fluorescence. We first assessed the range of Fe concentrations that stimulate nuclear accumulation of STOP1 in acidic condition (pH 5.5). Figure 4a (and Figure S4a for an independent experiment) shows that from 0 to 60 μM Fe GFP-fluorescence in the nuclei increases with Fe concentration; a plateau is reached around 60 μM Fe. Note that without Fe, we observe small fluorescent dots in cells (first picture in Figure 4a). These dots are autofluorescence of root cell components (i.e. not GFP fluorescence) since a WT seedling that does not carry the GFP marker displays similar dots (Figure S5).
Since in non-inducible conditions we do not detect GFP fluorescence in the cytoplasm, we hypothesized that the accumulation of GFP-STOP1 protein in the nucleus results from reduced proteasomal degradation (instead of i.e. translocation form cytosol). We then tested the effect of MG132, an inhibitor of the 26S proteasome, on the accumulation of GFP-STOP1 in seedlings grown in a moderate amount of Fe (Agar Sigma without addition of Fe, see Table S1). When treated with MG132, the GFP fluorescence substantially accumulated in the nucleus (Figure 4b, see also Figure S6 for additional pictures of two independent experiments). This result therefore supports the idea that Fe somehow inhibits the degradation of STOP1 by the 26S proteasome.

We then performed a kinetic analysis, at pH 5.5, of the nuclear accumulation of STOP1. Figure 4c (and Figure S4b) shows that in seedlings transferred in a medium without Fe added (-Fe), the level of nuclear GFP-fluorescence remains low through the 3 h of the kinetic. By contrast, after transfer of seedlings onto plates containing 60 μM Fe, the GFP fluorescence in nuclei increases after 30 min and becomes higher than in the -Fe control after 1h; and the fluorescence further increases with time. This confocal analysis, performed in -Pi condition for all conditions, indicates that Fe, and not the -Pi condition *per se*, rapidly promotes the accumulation of STOP1 in the nucleus.

We have shown previously that the acidity of the growth medium is a crucial parameter to stimulate *ALMT1* expression (Balzergue et al., 2017). We therefore tested whether low pH on its own also promotes the nuclear accumulation of STOP1. Figure 4d (and Figure S4c) shows that, indeed, in presence of 60 μM Fe, the level of nuclear GFP-fluorescence of GFP-STOP1 is higher in acidic conditions, whereas at pH 6.7 it is low and does not significantly differ from the -Fe control. This confirms the result shown in Figure 4a: an acidic pH (below 6.1) without Fe does not stimulate accumulation of GFP-STOP1 in the nucleus. These measures show that a low pH is required, but not sufficient, to stimulate nuclear accumulation of STOP1; the accumulation occurs only in acidic conditions supplemented with Fe. This comforts results shown in Figure 3 about the expression of *ALMT1*.

Aluminum triggers STOP1 accumulation in the nucleus

STOP1 and ALMT1 participate to resistance against Al^{3+} toxicity, and Al^{3+} stimulates the expression of *ALMT1*. As, for Fe (Figure 2b), in seedlings grown on plates made with the washed, DFO-treated agar, the expression of *ALMT1* is restored by addition of 15 μM Al^{3+} (Figure S7). We therefore asked whether Al^{3+} also stimulates STOP1 to accumulate in the nucleus. Seedlings were grown 3 days in agarose Seakem plates, and transferred for 2 h in plates supplemented or not with Al^{3+} before observing GFP-fluorescence of GFP-STOP1. Preliminary observations showed GFP-fluorescence in the nucleus after the transfer in Al-plates. A dose-response curve indicated that 15 μM Al^{3+} is sufficient to detect an accumulation of GFP in the nucleus, and a plateau is reached at about 30 μM Al^{3+} (Figure 5a and Figure S8a for an independent experiment). A kinetic indicates that 1 h after transfer the GFP signal is already significantly higher than the control not supplemented with Al (Figure 5b, Figure S8b). The signal further increases through the 3 h kinetic.

As for Fe, a low-pH (from 5.5 to 6.7) is required to Al to promote the nuclear accumulation of the GFP-STOP1 (Figure 5c and Figure S8c). These experiments show that Al, as Fe, rapidly triggers nuclear accumulation of STOP1 when the growth conditions are acidic.

The overaccumulation of STOP1 in root nuclei of *als3* is Fe-dependent

Using the *pSTOP1::GFP-STOP1* marker we previously shown that in the *als3* and *star1* mutants, the accumulation of GFP-STOP1 in root nuclei is much higher than in the WT (Wang et al., 2019). We thus asked whether this overaccumulation depends of Fe. We confirmed that, when grown on agarose Seakem plates supplemented with 60 μM Fe, the *als3* mutant accumulates much more GFP-STOP1 in nuclei than the WT control (Figure 6). In -Fe, this accumulation is suppressed in both the WT and the *als3* mutant (Figure 6). This result was confirmed with the DFO-agar (Figure S9). Therefore, the enhanced accumulation of nuclear GFP-STOP1 in *als3* root nuclei depends of Fe. Our results show that Fe is critical for STOP1 to accumulate in nucleus, and ALS3 repress this accumulation in a Fe-dependent manner.

Discussion

We, and others, have previously shown that several aspects of the root growth arrest under -Pi conditions are Fe-dependent (Svistoonoff et al., 2007, Ward et al., 2008, Dong et al., 2017, Muller et al., 2015, Gutiérrez-Alanís et al., 2017, Singh et al., 2018, Wang et al., 2019), but the relationships between -Pi and Fe were unclear. Here, we focused our work on the STOP1 signalling and succeed to dissociate the effect of -Pi itself from the role of Fe in the STOP1 signalling.

We compared the expression of *SPX1* and *PPsPase* genes as marker of the systemic -Pi stress with that of *ALMT1* that belongs to the local -Pi-stress. We show that, in the root, Fe stimulates the expression of *ALMT1* regardless the concentration of Pi, and the -Pi-Fe as well as the +Pi-Fe conditions decrease the expression of *ALMT1*. In addition, we demonstrate that the accumulation of STOP1 in root tip nuclei is Fe-dependent. By contrast, the expression of *SPX1* and *PPsPase* happens only under the -Pi condition and it is not correlated with the availability of Fe in the medium (Figure 3 and Figure S2). Supporting this conclusion, our previous results showed that the expression of *ALMT1* in -Pi does not depend of PHR1 and PHL1 genes (Balzergue et al., 2017), two targets of SPX1 regulation (Puga et al., 2014).
We thus demonstrate that, under -Pi conditions, it is the Fe and not the -Pi condition itself that stimulates the accumulation of STOP1 in root nuclei and the transcription of *ALMT1*. Under +Pi, Fe is probably associated with Pi molecules, thus hampering the Fe-dependent regulation of nuclear STOP1 and the catalysis of ROS production, whereas under -Pi condition, Fe is more available to stimulate these two processes.
Therefore, the STOP1 signalling pathway is clearly distinct from the systemic -Pi signalling, at least the PHR1- and PHL1-dependent pathway.

Fe and Al stimulate the accumulation of STOP1 in the nucleus

Our work demonstrates that Fe and Al^{3+} stimulate the accumulation of STOP1 in the nucleus. In previous works by others, the cellular localisation of Arabidopsis STOP1 and STOP1 homologues was assessed by transient expression in onion cells, Arabidopsis protoplasts, protoplasts derived from rice callus, tobacco leaves or *Nicotiana benthamiana* leaves. In all these assays, the STOP1 proteins, fused to the GFP, were localized in the nucleus (Sawaki et al., 2009, Sawaki et al., 2014, Fan et al., 2015, Daspute et al., 2018, Huang et al., 2018, Wang et al., 2017, Wu et al., 2018, Yamaji et al., 2009, Che et al., 2018). In these assays, the growth media used were not phosphate deficient or particularly enriched in Fe or Al^{3+}. This suggests that, in these experimental conditions, the pathway stimulating or repressing the accumulation of STOP1 in the nucleus is constitutively active or inactive, respectively. Supporting this last idea, an immunostaining experiment showed a constitutive nuclear localization of OsART1 in WT root cells (i.e. not affected by Al treatment) (Yamaji et al., 2009). Another possibility is that overexpression of the STOP1 protein saturates the putative regulatory mechanism governing its nuclear accumulation. Alternatively, these STOP1 proteins are differently regulated in these cells compared to the root cells of Arabidopsis.

In the past, we have shown that under neutral pH condition the root growth is not arrested in low-Pi (Svistoonoff et al., 2007) and *ALMT1* is not expressed (Balzergue et al., 2017). These two phenomena are now explained (at least partially) as we show that under low-pH without Fe or Al^{3+}, STOP1 does not accumulate in the nucleus and, reciprocally, in the presence of Fe or Al^{3+}, but at pH 6.7 STOP1 does not accumulate in the nucleus either (Figures 4 and 5). The low pH is thus a necessary but not sufficient condition to stimulate nuclear STOP1.
Our qRT-PCR result shows that *IRT1* — a gene whose expression is induced when Fe is poorly available, like on the DFO-agar (Figure 3b) — is not or poorly induced at pH 6.7 (Figure 3b, agar Sigma and agarose Seakem), indicating that seedlings are not Fe-deficient. Nevertheless, this pH prevents the accumulation of STOP1 in the nucleus. This suggests that different Fe signalling or different pools or forms of Fe regulate *IRT1* expression and STOP1 nuclear accumulation. Knowing that $Fe^{2/3+}$ and

Al^{3+} are soluble only under low pH, STOP1 regulation seems sensitive to the cationic form of Fe and Al.

The first *stop1* mutant was originally identified for its defective root growth on agar plates made with a MS medium at pH 4.3 (Iuchi et al., 2007). The authors confirmed the hypersensitivity to low-pH by using hydroponic culture; this growth medium contained only submicromolar concentration of Fe (and no Pi). According to the results presented here, under acidic conditions without Fe (or Al^{3+}), STOP1 poorly accumulates in the nucleus. Then, if STOP1 does not accumulate in nucleus under these growth conditions, how does it participate to resistance against low-pH? One hypothesis is that a very low amount of Fe, at pH 4.3, is sufficient to stimulate the accumulation of STOP1 for triggering the expression of genes for H^+ tolerance. Alternatively, STOP1 might have already started promoting the expression of genes involved in H^+ tolerance before (i.e. during embryogenesis) seedlings encounter acidic conditions. A transcriptomic study on seedlings grown in acidic environment shown that *stop1* mutant is defective for the expression of several genes, including genes involved in cell wall composition or modelling (Sawaki et al., 2009). Furthermore, physiological studies suggested that *stop1* seedlings are defective in a mechanism alleviating H^+ toxicity, via perhaps Ca^{2+} stabilization of the cell wall (Kobayashi et al., 2013b). It is therefore tempting to speculate that already during WT embryogenesis, STOP1 participates in the making of root cells with a cell wall able to tolerate H^+ during few days after germination, and in the *stop1* seeds the root cell wall are somehow altered, leading to reduced root growth under acidic conditions.

ALS3 and STAR1 repress the accumulation of STOP1 in the nucleus

In a previous work, Wang et al demonstrated that, together, ALS3 and STAR1 repress the accumulation of STOP1 in the nucleus (Wang et al., 2019). ALS3 and STAR1 associate to form an ABC-type transporter located in the tonoplast. We thus inferred a model whereby a cytosolic metabolite stimulates the accumulation of STOP1 in the nucleus, and that ALS3-STAR1 transporter pumps this metabolite from the cytosol to the vacuole. According to this model, the cytosolic concentration of this metabolite is higher in *als3* and *star1* mutants than in WT, thereby increasing nuclear STOP1.

We showed here that the overaccumulation of STOP1 in the nucleus of *als3* mutant is abrogated when the seedling grows in a Fe-depleted medium (Figure 6). Since our results on the nuclear STOP1 with Al^{3+} are similar to those with Fe, this metabolite could be the trivalent metal (Fe^{3+} or Al^{3+}) or a Fe (or Al^{3+})-containing molecule. This hypothesis would fit with the role of ALS3-STAR1 in Al^{3+} tolerance. However, we cannot exclude that this metabolite does not contain Fe (or Al^{3+}).

The *STOP1*, *ALS3* and *STAR1* genes are all expressed in the root tip (Larsen et al., 2005, Dong et al., 2017, Balzergue et al., 2017, Mora-Macias et al., 2017); this is coherent with their role as a shared functional unit.

The two effects of Fe on root growth arrest

A two-branched regulatory pathway modulates the root growth arrest: the STOP1/ALMT1/ALS3/STAR1 branch and the LPR1/PDR2 branch (Balzergue et al., 2017, Abel, 2017, Wang et al., 2019). These two branches are converging on the Fe-dependent production of ROS in the cell wall. In the *lpr1* mutant the expression of *ALMT1* is not altered compared to WT (Balzergue et al., 2017). This means that in

the *lpr1* mutant, STOP1 is as active as in the WT. Since the *lpr1* root tip accumulates far less extracellular Fe and ROS than in the WT, ROS and extracellular Fe seem not crucial for activating STOP1 for *ALMT1* expression. Instead, our present work with ALS3 indicates that an intracellular metabolite (containing Fe or Al^{3+}?) activates the STOP1 branch.

In Figure 7 a model summarizes our current knowledge of this two-branched pathway. The phosphate ions inactivate Fe by forming a complex with it. Under -Pi condition, Fe is released from this complex. Fe –or an unknown compound– accumulates in the cell where it stimulates the accumulation of STOP1 in the nucleus by inhibiting its proteasomal degradation. Inside the nucleus STOP1 activates the transcription of *ALMT1*. The ALMT1 protein exudes malate in the apoplast where, together with Fe and the ferroxidase LPR1, they generate ROS that inhibit cell wall expansion via the cross-linking activity of cell wall peroxidases. In the tonoplastic membrane, ALS3 and STAR1 pump Fe –or the unknown compound– from the cytosol to the vacuole compartment. It follows that the concentration of Fe, or the unknown compound, in the cytosol decreases and this reduces the accumulation of STOP1 in the nucleus, and therefore reduces also the expression of *ALMT1*.

Note that Fe has two effects: it directly or indirectly activates the accumulation of STOP1 in the nucleus and it also participates to the generation of ROS in the apoplast. These two effects can be uncoupled; for example, the *lpr1* mutant still expresses *ALMT1* but its root growth is not inhibited under -Pi.

For the aluminium, the model only partially applies because the exuded malate prevents the inhibitory effect of toxic Al^{3+} on root growth. In addition, we do not know whether ALS3 and STAR1 pump Al^{3+}. In any case, Fe and Al^{3+} share several characteristics in the nuclear accumulation of STOP1: dependency to low-pH, similar kinetics, negative role of ALS3-ASTAR1. This could mean that Fe and Al^{3+} have some common signalling steps activating STOP1. Many points remain obscure or not yet demonstrated in this model. In particular, how cellular Fe (and Al^{3+}) regulates STOP1.

How the Fe and Al stimulate STOP1 accumulation in nucleus?

In plants, few Fe-sensing proteins have been identified (Kobayashi & Nishizawa, 2012). The HRZ (Haemerythrin motif-containing Really Interesting New Gene (RING)-and Zinc-finger) proteins BRUTUS (BTS), BTS-like, OsHRZ1 and OsHRZ2 are E3 ligases involved in the low-Fe response (Kobayashi et al., 2013a, Long et al., 2010, Hindt et al., 2017). They target to proteasomal degradation several basic helix-loop-helix transcription factors like the POPEYE (PYE) and PYE-like such as bHLH104 and bHLH105, which are positive regulators of the low-Fe response. Under Fe-sufficient condition, the binding of Fe to the hemerythrin domains destabilizes the HRZ proteins, thereby relieving the transcriptional response to low-Fe (Selote et al., 2015, Kobayashi et al., 2013a). Also involved in transcriptional regulation of the Fe-homeostasis are the IDEF1 and IDEF2 proteins that bind Fe, as well as zinc (Kobayashi et al., 2012).

Here we have shown that MG132, an inhibitor of the 26S proteasome, substantially increases the level of GFP-STOP1 accumulated in the nucleus in seedlings grown in poorly inductive conditions (i.e. low-Fe; Figure 4b and Figure S6). This indicates that under poorly or non-inductive conditions, STOP1 is degraded by the 26S-proteasome pathway. Recently, Zhang et al. (Zhang et al., 2019) found an F-box protein, RAE1, promoting the degradation of STOP1 via the 26S-proteasome pathway. The REA1 protein interacts with and triggers the 26S-proteasome-dependent degradation of

STOP1. Compared to the WT, seedlings homozygous for the loss-of-function *rae1* mutation accumulate more STOP1 proteins and *ALMT1* mRNAs. When grown under -Pi condition, the *rae1* seedlings have a primary root shorter than that of the WT, and when grown with toxic amount of Al it is longer. RAE1 is therefore a strong candidate mediating STOP1 degradation in our Fe- and Al-depleted growth conditions.

The RAE1 and STOP1 proteins do not contain an obvious Fe- or Al-binding domain. How Al^{3+} is sensed in plant is not known (Kochian et al., 2015) and thus the activation of STOP1 by Al^{3+} remains an open question. But, since both Fe and Al^{3+} stimulate the accumulation of STOP1 in the nucleus with similar kinetics, in the same root cells and only under acidic conditions, it is tempting to speculate that these two cations share a sensing mechanism. Further work will be needed to understand this mechanism.

Conclusion

In acidic soils, toxic Al^{3+} and Fe, in conjunction with Pi-deficiency limit crops growth (Kochian, 2004). There are increasing evidences that, at the cellular level, toxic Al^{3+} share some common targets and processes with the effects of Fe cations in acidic and low-Pi conditions (Abel, 2017). We now demonstrate that Al^{3+} and Fe also share at least one signalling step: STOP1 accumulation in the nucleus. Our study therefore contributes to further dissection of the sensing and signalling pathways of Al and Fe in plants.

Experimental procedures

Plant material.

The Arabidopsis wild-type (Col^{er105}), *pALMT1::GUS*$_{\#2}$, *pSTOP1::GFP-STOP1*$_{\#B10}$ and *als3*; *pSTOP1::GFP-STOP1*$_{\#B10}$ lines were described previously (Balzergue et al., 2017, Wang et al., 2019); *pSPX1::GUS* is in the Col-0 background (Duan et al., 2008).

Seedling growth.

Seeds were surface-sterilised 5 min in a solution containing 70% ethanol and 0.05% sodium dodecyl sulfate, and washed twice with ethanol 96%. The nutrient solution was as previously (Balzergue et al., 2017). The agar (8 g l^{-1}) and agarose (7 g l^{-1}) for plates was from Sigma-Aldrich (A1296 #BCBL6182V) and Lonza (Seakem LE agarose) respectively. The media were buffered at pH ranging from 5.5-6.8 with 3.4 mM 2-(*N*-morpholino) ethane sulfonic acid. The different plates were prepared by mixing the melted autoclaved 1X agar or agarose medium (composition as above) with the buffer. Solutions of $AlCl_3$ and $FeCl_2$ were sterilized by filtration before adding to the plates.

For GFP fluorescence experiments, five seeds were sown on a piece of sterile nylon square (1 cm X 1 cm, mesh size 10 μm) itself lying on the agar plate. After 3 days of growth on the agar plate, the nylon meshes carrying the seedlings were transferred on the new plates containing or not different concentrations of aluminium or iron.

For the experiments with MG132, nylon meshes carrying the 3 days old seedlings were transferred on 10 µl droplet (liquid extracted from Sigma-Aldrich agar (A1296 #BCBL6182V) from which the seedlings were pre-grown) containing or not different

concentration of MG132. In all experiments, the pH of the growth media for germination and for the subsequent transfer was identical.

For the qRT–PCR experiment, seeds were sown side by side in a line, on a 5 cm strip of nylon meshes. Three to 3.5 days after sowing the whole roots of seedlings were harvested and mRNA extracted.

Agar treatment with deferoxamine B (DFO)

To reduce bioavailable iron in the growth media, we used two methods. For the DFO-agar, 100 µM of deferoxamine B (DFO) was added to the 1x melted autoclaved growth media, just before pouring the plates. For the washed DFO-treated agar, we prepared the agar as follow: 4 g of Sigma-Aldrich agar (A1296 #BCBL6182V) was added to 100 ml of milliQ water containing 600 µM of DFO and stirred during 15 h. The agar was then washed by centrifugation (520 rcf) through a nylon mesh (mesh size 10 µm); this washing step with milliQ water was carried out twice. This washed DFO-agar was then used to prepare the growth plates.

Quantification of Al, Fe and P in the agars and agarose

Dried samples of agars and agarose were mineralized by addition of 300 µL HNO_3 70% (ICP grade, JT Baker) by incubation overnight in an oven at 80 °C. The solutions were diluted to a final volume of 5 mL by addition of distilled water. The Al, Fe and P were quantified with Inductively Coupled Plasma – Absorption Emission Spectrometer (ICP-AES 5110 SVDV, Agilent Technologies). The concentrations of metals were determined using standard curves obtained from solutions made with ICP-grade elements.

Quantitative RT–PCR.

Total RNA were extracted from whole roots using the Direct-Zol™ RNA MiniPrep (ZYMO research, USA) and treated with the RNase-free DNase Set (ZYMO research, USA) according to the manufacturer's instructions. Reverse transcription was performed on 500 ng of total RNA using the qScript™ cDNA SuperMix (Quanta Bioscience™). Quantitative PCR (qRT–PCR) was performed on a 480 LightCycler thermocycler (Roche) using the manufacturer's instructions with Light cycler 480sybr green I master (Roche) and with primers listed in Table S2. We used Tubulin gene (At5g62690) as a reference gene for normalization and the quantification of gene expression was as according the published method (Pfaffi, 2001).

GUS histochemical staining.

The GUS staining of Arabidopsis seedlings was conducted as previously described (Balzergue et al., 2017), except that the seedlings were incubated 40 min in the GUS staining solution.

Quantification of GFP fluorescence.

Images were collected on a Zeiss LSM780 confocal microscope (Carl Zeiss, France) using a × 20 dry objective (Plan Apo NA 0.80). GFP were excited with the argon ion laser (488 nm). Emitted light was collected from 493 to 538 nm for GFP, using the MBS 488 filter. All nuclei were imaged using the same conditions of gain, offset, resolution and with a pinhole setting of 1 a.u. The quantification of GFP fluorescence was carried out as follows: a Z-stack of 9 images (separated by 1.8 µm distance) imaged representative nuclei on the surface of the root. Images were acquired in 12

bits using Zen black software (Zen black 2012 SP2 Version 11.0), then converted to a maximal projection image. The average nuclei fluorescence intensities were quantified using the Zen blue software (Zen 2 blue edition, version 2.0.0.0), by drawing identical ROI (region of interest). A 120 µm X 60 µm rectangle was defined at 200 µm from a root tip (roughly in the transition zone), in which a region of interest (6 µm X 6 µm) inside each nucleus was defined for the measurement of fluorescence.

Acknowledgements

B.Alonso, S.Chiarenza, H.Javot and N.Léonhardt (CEA, cadarache) for experimental helps and discussions.
This work was funded by CEA, Investissements d'avenir (DEMETERRES) and ROULLIER/AGRO INNOVATION INTERNATIONAL (C.M.); X.W. and D.L. were funded by The National Natural Science Foundation of China (grant no. 31670256). Support for the microscopy equipment was provided by the Région Provence Alpes Côte d'Azur, the Conseil General of Bouches du Rhône, the French Ministry of Research, the CNRS and the Commissariat à l'Energie Atomique et aux Energies Alternatives. The qRT-PCR machine was funded by Héliobiotech.
The authors declare no competing interests.

Short legends for Supporting Information

Figure S1
Under neutral condition, *ALMT1* is not expressed.
Picture of the root tip after the GUS staining, of WT seedlings carrying the *pALMT1::GUS* marker. Seedlings were grown in low-Pi at pH 5.8 or 7.1, with or without 15 µM Fe. Note that at pH 7.1 no GUS staining is detected. Bar, 1 mm.

Figure S2
Expression (qRT-PCR) of *ALMT1*, *SPX1* and *PPsPase* in seedlings roots. Seedlings were grown 3 days on the indicated media. Mean +/-SD (*n* = two independent experiments).

Figure S3
Analysis of *STOP1* mRNA expression.
WT seedlings were pre-grown 3 days under low-Pi condition at pH 5.8 or 7 without Fe or Al added, transferred for 3 hours in the same original pH condition with or without Al^{3+} or Fe^{2+} before extraction of root RNAs and qRT-PCR reactions. The conditions for qRT-PCR reactions and the calculations of relative expression were as in Figure 3 and Figure S2. Mean +/-SD (*n* = two independent experiments). *ALMT1* was used as a control.

Figure S4
Fe promotes the accumulation of GFP-STOP1 in root nuclei.

The GFP fluorescence was measured (a.u.) in nuclei at the root tip of *pSTOP1::GFP-STOP1* seedlings.
a) Three-day-old seedlings were transferred 2 h in -Pi plates with the indicated concentration of Fe.

b) Three-day-old seedlings were transferred for the indicated time in -Pi plates containing 0 or 60 μM Fe.
c) Three-day-old seedlings were transferred 2h in -Pi plates buffered at the indicated pH, containing 0 or 60 μM Fe.
d) Picture of GFP fluorescence at the root tip, in seedlings transferred 2h in -Pi plates without (left) or with (right) 60 μM Fe.

Box plots indicate the median, the 25th to 75th percentiles (box edges) and the min to max range (whiskers); Mann-Whitney test; ****P<0.0001; NS, not significant (P>0.05); number of nuclei per condition: a) 329-346; b) 291-343; c) 322-392).

Figure S5
Non-transgenic WT seedlings were grown on a -Pi-Fe plate made with the DFO-agar, transferred to a –Pi plate containing 0 or 60 μM Fe for 2 h, and the fluorescence pictured by confocal microscopy (same setting as in Figure S9). Note the small autofluorescent dots. Bar, 100 μm.

Figure S6
The 26S proteasome inhibitor MG132 promotes GFP-STOP1 accumulation in root nuclei.
Three days old seedlings were treated 6 h (a) or 4 h (b), without or with 60, 125 or 250 μM (a) or 250 μM (b) MG132, and photographed as in Figure 4b. **a** and **b** represent two independent experiments. Bars, 100 μm.

Figure S7
Aluminum stimulates the expression of *pALMT1::GUS*.

Seedlings were grown four days on a -Pi medium pH 5.5, made with a washed DFO-treated agar, supplemented or not with 15 μM Al^{3+}, before GUS staining. Note that the 0 Al control is the same as in Figure 2b, since it is part of the same experiment. Bar, 1 mm.

Figure S8
Al^{3+} promotes the accumulation of GFP-STOP1 in root nuclei.

The GFP fluorescence was measured (a.u.) in nuclei at the root tip of pSTOP1::GFP-STOP1 seedlings.
a) Three-day-old seedlings were transferred 2 h in -Pi plates with the indicated concentration of Al^{3+}.
b) Three-day-old seedlings were transferred for the indicated time in -Pi plates containing 0 or 30 μM Al^{3+}.
c) Three-day-old seedlings were transferred 2h in -Pi plates buffered at the indicated pH, containing 0 or 30 μM Al^{3+}.

Box plots indicate the median, the 25th to 75th percentiles (box edges) and the min to max range (whiskers); Mann-Whitney test; ****P<0.0001; number of nuclei per condition: a) 315-348; b) 330-399; c) 315-448).

Figure S9
ALS3 represses STOP1 accumulation in root nuclei.

a) WT and the *als3* mutant seedlings carrying the *pSTOP1::GFP-STOP1* construct were grown 3 days on a -Pi-Fe plate, transferred to -Pi or -Pi-Fe plates for 2 h, and GFP-fluorescence was pictured by confocal microscopy. Bars, 100 μm.

References

Abel S, 2017. Phosphate scouting by root tips. *Curr Opin Plant Biol* **39**, 168-77.

Balzergue C, Dartevelle T, Godon C*, et al.*, 2017. Low phosphate activates STOP1-ALMT1 to rapidly inhibit root cell elongation. *Nat Commun* **8**, 15300.

Bouain N, Shahzad Z, Rouached A*, et al.*, 2014. Phosphate and zinc transport and signalling in plants: toward a better understanding of their homeostasis interaction. *J Exp Bot.* **65**, 5725-41.

Briat JF, Rouached H, Tissot N, Gaymard F, Dubos C, 2015. Integration of P, S, Fe, and Zn nutrition signals in Arabidopsis thaliana: potential involvement of PHOSPHATE STARVATION RESPONSE 1 (PHR1). *Front Plant Sci* **6**, 290.

Che J, Tsutsui T, Yokosho K, Yamaji N, Ma JF, 2018. Functional characterization of an aluminum (Al)-inducible transcription factor, ART2, revealed a different pathway for Al tolerance in rice. *New Phytol* **220**, 209-18.

Daspute AA, Kobayashi Y, Panda SK*, et al.*, 2018. Characterization of CcSTOP1; a C2H2-type transcription factor regulates Al tolerance gene in pigeonpea. *Planta* **247**, 201-14.

Dong J, Pineros MA, Li X*, et al.*, 2017. An Arabidopsis ABC Transporter Mediates Phosphate Deficiency-Induced Remodeling of Root Architecture by Modulating Iron Homeostasis in Roots. *Mol Plant* **10**, 244-59.

Duan K, Yi K, Dang L, Huang H, Wu W, Wu P, 2008. Characterization of a sub-family of Arabidopsis genes with the SPX domain reveals their diverse functions in plant tolerance to phosphorus starvation. *Plant J* **54** 965–75.

Fan W, Lou HQ, Gong YL*, et al.*, 2015. Characterization of an inducible C2H2-type zinc finger transcription factor VuSTOP1 in rice bean (Vigna umbellata) reveals differential regulation between low pH and aluminum tolerance mechanisms. *New Phytologist* **208**, 456-68.

Gutiérrez-Alanís D, Yong-Villalobos L, Jiménez-Sandoval P*, et al.*, 2017. Phosphate Starvation-Dependent Iron Mobilization Induces CLE14 Expression to Trigger Root Meristem Differentiation through CLV2/PEPR2 Signaling. *Dev Cell* **41**, 555–70.

Hanchi M, Thibaud MC, Legeret B*, et al.*, 2018. The Phosphate Fast-Responsive Genes PECP1 and PPsPase1 Affect Phosphocholine and Phosphoethanolamine Content. *Plant Physiol* **176**, 2943-62.

Hindt MN, Akmakjian GZ, Pivarski KL*, et al.*, 2017. BRUTUS and its paralogs, BTS LIKE1 and BTS LIKE2, encode important negative regulators of the iron deficiency response in Arabidopsis thaliana. *Metallomics* **9**, 876-90.

Hinsinger P, 2001. Bioavailability of soil inorganic P in the rhizosphere as affected by root-induced chemical changes: a review. *Plant soil* **237**, 173-95.

Hirsch J, Marin E, Floriani M*, et al.*, 2006. Phosphate deficiency promotes modification of iron distribution in Arabidopsis plants. *Biochimie* **88**, 1767-71.

Hoekenga OA, Maron LG, Pineros MA*, et al.*, 2006. AtALMT1, which encodes a malate transporter, is identified as one of several genes critical for aluminum tolerance in Arabidopsis. *Proc Natl Acad Sci U S A* **103**, 9738-43.

Huang CF, Yamaji N, Ma JF, 2010. Knockout of a bacterial-type ATP-binding cassette transporter gene, AtSTAR1, results in increased aluminum sensitivity in Arabidopsis. *Plant Physiol* **153**, 1669-77.

Huang S, Gao J, You J*, et al.*, 2018. Identification of STOP1-Like Proteins Associated With Aluminum Tolerance in Sweet Sorghum (Sorghum bicolor L.). *Front Plant Sci* **9**, 258.
Iuchi S, Koyama H, Iuchi A*, et al.*, 2007. Zinc finger protein STOP1 is critical for proton tolerance in Arabidopsis and coregulates a key gene in aluminum tolerance. *Proc Natl Acad Sci U S A* **104**, 9900-5.
Kobayashi T, Itai RN, Aung MS, Senoura T, Nakanishi H, Nishizawa NK, 2012. The rice transcription factor IDEF1 directly binds to iron and other divalent metals for sensing cellular iron status. *Plant J* **69**, 81-91.
Kobayashi T, Nagasaka S, Senoura T, Itai RN, Nakanishi H, Nishizawa NK, 2013a. Iron-binding haemerythrin RING ubiquitin ligases regulate plant iron responses and accumulation. *Nat Commun* **4**, 2792.
Kobayashi T, Nishizawa NK, 2012. Iron uptake, translocation, and regulation in higher plants. *Annu Rev Plant Biol* **63**, 131-52.
Kobayashi Y, Kobayashi Y, Watanabe T*, et al.*, 2013b. Molecular and physiological analysis of Al^{3+} and H^{+} rhizotoxicities at moderately acidic conditions. *Plant Physiol* **163**, 180-92.
Kochian LV, Hoekenga, O. A., Pineros, M. A., 2004. How do crop plants tolerate acid soils? Mechanisms of aluminum tolerance and phosphorous efficiency. *Annu Rev Plant Biol.* **55**, 459-93.
Kochian LV, Pineros MA, Liu JP, Magalhaes JV, 2015. Plant Adaptation to Acid Soils: The Molecular Basis for Crop Aluminum Resistance. *Annu Rev Plant Biol.* **66**, 571-98.
Larsen PB, Geisler MJ, Jones CA, Williams KM, Cancel JD, 2005. ALS3 encodes a phloem-localized ABC transporter-like protein that is required for aluminum tolerance in Arabidopsis. *Plant J.* **41**, 353-63.
Long TA, Tsukagoshi H, Busch W, Lahner B, Salt DE, Benfey PN, 2010. The bHLH transcription factor POPEYE regulates response to iron deficiency in Arabidopsis roots. *Plant Cell* **22**, 2219-36.
Lynch JPB, K.M., 2001. Topsoil foraging - an architectural adaptation of plants to low phosphorus availability. *Plant and Soil* **237**, 225-37.
Misson J, Raghothama KG, Jain A*, et al.*, 2005. A genome-wide transcriptional analysis using Arabidopsis thaliana Affymetrix gene chips determined plant responses to phosphate deprivation. *Proc Natl Acad Sci U S A* **102**, 11934-9.
Mora-Macias J, Ojeda-Rivera JO, Gutierrez-Alanis D*, et al.*, 2017. Malate-dependent Fe accumulation is a critical checkpoint in the root developmental response to low phosphate. *Proc. Nat. Aca. Sci. USA* **114**, E3563-E72.
Muller J, Toev T, Heisters M*, et al.*, 2015. Iron-dependent callose deposition adjusts root meristem maintenance to phosphate availability. *Dev Cell* **33**, 216-30.
Pfaffi MW, 2001. A new mathematical model for relative quantification in real-time RT-PCR. *Nucleic Acids Res.* **29**, e45.
Puga MI, Mateos I, Charukesi R*, et al.*, 2014. SPX1 is a phosphate-dependent inhibitor of PHOSPHATE STARVATION RESPONSE 1 in Arabidopsis. *Proc Natl Acad Sci U S A* **111**, 14947-52.
Puga MI, Rojas-Triana M, De Lorenzo L, Leyva A, Rubio V, Paz-Ares J, 2017. Novel signals in the regulation of Pi starvation responses in plants: facts and promises. *Curr Opin Plant Biol* **39**, 40-9.
Reymond M, Svistoonoff S, Loudet O, Nussaume L, Desnos T, 2006. Identification of QTL controlling root growth response to phosphate starvation in Arabidopsis thaliana. *Plant Cell Environ* **29**, 115-25.

Sawaki Y, Iuchi S, Kobayashi Y, *et al.*, 2009. STOP1 regulates multiple genes that protect arabidopsis from proton and aluminum toxicities. *Plant Physiol* **150**, 281-94.
Sawaki Y, Kobayashi Y, Kihara-Doi T, *et al.*, 2014. Identification of a STOP1-like protein in Eucalyptus that regulatestranscription of Al tolerance genes. *Plant Sci.* **223**, 8-15.
Selote D, Samira R, Matthiadis A, Gillikin JW, Long TA, 2015. Iron-binding E3 ligase mediates iron response in plants by targeting basic helix-loop-helix transcription factors. *Plant Physiol* **167**, 273-86.
Singh AP, Fridman Y, Friedlander-Shani L, Tarkowska D, Strnad M, Savaldi-Goldstein S, 2014. Activity of the brassinosteroid transcription factors BRASSINAZOLE RESISTANT1 and BRASSINOSTEROID INSENSITIVE1-ETHYL METHANESULFONATE-SUPPRESSOR1/BRASSINAZOLE RESISTANT2 blocks developmental reprogramming in response to low phosphate availability. *Plant Physiol* **166**, 678-88.
Singh AP, Fridman Y, Holland N, *et al.*, 2018. Interdependent Nutrient Availability and Steroid Hormone Signals Facilitate Root Growth Plasticity. *Dev Cell* **46**, 59-72 e4.
Svistoonoff S, Creff A, Reymond M, *et al.*, 2007. Root tip contact with low-phosphate media reprograms plant root architecture. *Nat Genet* **39**, 792-6.
Thibaud MC, Arrighi JF, Bayle V, *et al.*, 2010. Dissection of local and systemic transcriptional responses to phosphate starvation in Arabidopsis. *Plant J* **64**, 775-89.
Ticconi CA, Delatorre CA, Lahner B, Salt DE, Abel S, 2004. Arabidopsis pdr2 reveals a phosphate-sensitive checkpoint in root development. *Plant J* **37**, 801-14.
Ticconi CA, Lucero RD, Sakhonwasee S, *et al.*, 2009. ER-resident proteins PDR2 and LPR1 mediate the developmental response of root meristems to phosphate availability. *Proc Natl Acad Sci U S A* **106**, 14174-9.
Vert G, Grotz N, Dedaldechamp F, *et al.*, 2002. IRT1, an Arabidopsis transporter essential for iron uptake from the soil and for plant growth. *Plant Cell* **14**, 1223-33.
Wang JJ, Hou QQ, Li PH, *et al.*, 2017. Diverse functions of multidrug and toxin extrusion (MATE) transporters in citric acid efflux and metal homeostasis in Medicago truncatula. *Plant Journal* **90**, 79-95.
Wang X, Wang Z, Zheng Z, *et al.*, 2019. Genetic Dissection of Fe-Dependent Signaling in Root Developmental Responses to Phosphate Deficiency. *Plant Physiol* **179**, 300-16.
Ward JT, Lahner B, Yakubova E, Salt DE, Raghothama KG, 2008. The effect of iron on the primary root elongation of Arabidopsis during phosphate deficiency. *Plant Physiol* **147**, 1181-91.
Wu W, Lin Y, Chen Q, *et al.*, 2018. Functional Conservation and Divergence of Soybean GmSTOP1 Members in Proton and Aluminum Tolerance. *Front Plant Sci* **9**, 570.
Yamaji N, Huang CF, Nagao S, *et al.*, 2009. A zinc finger transcription factor ART1 regulates multiple genes implicated in aluminum tolerance in rice. *Plant Cell* **21**, 3339-49.
Zhang Y, Zhang J, Guo J, *et al.*, 2019. F-box protein RAE1 regulates the stability of the aluminum-resistance transcription factor STOP1 in Arabidopsis. *Proc Natl Acad Sci U S A* **116**, 319-27.

Table S1: Al, Fe and P content (μg/100 mg agar or agarose)

	Al	Fe	P
Agar Sigma A1296	5,75	3,82	5,86
Agar Sigma A1296 treated with DFO and washed	5,87	3,50	0,63
Agarose lonza Seakem	0,42	0,24	0,81

Table S2: primers sequence

gene	primer	sequence (5' to 3')
PPsPase1	AT1G73010_R	GACGACACGTGGATGAATTG
	AT1G73010_F	TCATGATCAAGGCAAAACCA
SPX1	AT5G20150_R	GCGGCAATGAAAACACACTA
	AT5G20150_F	CGGGTTTTGAAGGAGATCAG
IRT1	AT4G19690_R	GACGATAGAACTATACTGCCTTGA
	AT4G19690_F	TGCGGAATTGAAATCATGTG
ALMT1	AT1G08430_R	CGATTCCGAGCTCATTCTTC
	AT1G08430_F	GGCAGTGTGCCTACAGGATT
STOP1	AT1G34370_F	AAGTGGCTTTGTTCCTGTGG
	AT1G34370_R	GGCTGTGTGGTTTCTTGGTT
Tubulin	AT5G62690_R	ACACCAGACATAGTAGCAGAAATCAAG
	AT5G62690_F	GAGCCTTACAACGCTACTCTGTCTGTC

Figure legends

Figure 1

Antagonistic interactions of Pi and Fe on the expression of *pALMT1::GUS*.
a) Effect of the Pi concentration on GUS staining, when Fe is at 15 μM.
b) Effect of the Fe concentration on GUS staining, when Pi is at 250 μM.
Seedling were grown 3 days on a pH 6.7 medium not supplemented with Pi and Fe, and transferred 24 h on a pH 5.5 medium supplemented with the indicated concentrations of Pi and Fe, before GUS staining. Bar, 1 mm.

Figure 2

Fe is necessary for the expression of *ALMT1*.
a) DFO inhibits the expression of *pALMT1::GUS*.
b) In a growth medium made with a washed DFO-treated agar, supplementation of Fe restores the expression of *pALMT1::GUS*.
Seedling were grown 4 days on a pH 5.5 medium not supplemented with Pi, and supplemented or not with the indicated concentrations of DFO and Fe, before GUS staining. Bar, 1 mm.

Figure 3

Fe, but not the -Pi condition *per se*, stimulates the expression of *pALMT1::GUS*.
a) GUS staining in the primary root of *pALMT1::GUS* and *pSPX1::GUS* seedlings.
b) Expression (qRT-PCR) of *ALMT1*, *SPX1*, *IRT1* and *PPsPase* in seedlings roots (mean of three technical replicates).

Seedlings were grown 5 days (for the GUS staining experiment) or 3.5 days (for the qRT-PCR experiment) on a medium not supplemented with Pi and Fe, at pH 6.7 or 5.5. Bars, 1 mm.

Figure 4
Fe promotes the accumulation of GFP-STOP1 in root nuclei

The GFP fluorescence was measured (a.u.) in nuclei at the root tip of *pSTOP1::GFP-STOP1* seedlings.
a) Top: three-day-old seedlings were transferred 2 h in -Pi plates with the indicated concentration of Fe. Bottom: representative pictures used for measurements.

b) MG132 promotes the accumulation of GFP-STOP1 in nuclei of the root tip. Seedlings carrying the *pSTOP1::GFP-STOP1* reporter were grown 3 days in agar (Agar Sigma A1296, Table S1). under low-Pi without Fe or Al added. Then, they were treated 4 h with or without 250 μM MG132 before photographed with the confocal microscope. One representative picture is shown for each condition (see Figure S6 for additional pictures). Note that under in the untreated control, STOP1 slightly accumulates in the nucleus.
c) Left: three-day-old seedlings were transferred for the indicated time in -Pi plates containing 0 or 60 μM Fe. Right: representative pictures used for measurements.
d) Top: three-day-old seedlings were transferred 2 h in -Pi plates buffered at the indicated pH, containing 0 or 60 μM Fe. Bottom: representative pictures used for measurements.

Box plots indicate the median, the 25th to 75th percentiles (box edges) and the min to max range (whiskers); Mann-Whitney test; ****P<0.0001; ***P<0.001; *P<0.5; NS, not significant (P>0.05); number of nuclei per condition: a) 94-154; b) 99-119; c) 87-121). Bars, 100 μm.

Figure 5
Al^{3+} promotes the accumulation of GFP-STOP1 in root nuclei.

The GFP fluorescence was measured (a.u.) in nuclei at the root tip of *pSTOP1::GFP-STOP1* seedlings.
a) Top: three-day-old seedlings were transferred 2 h in -Pi plates with the indicated concentration of Al^{3+}. Bottom: representative pictures used for measurements.
b) Left: three-day-old seedlings were transferred for the indicated time in -Pi plates containing 0 or 30 μM Al^{3+}. Right: representative pictures used for measurements.
c) Top: three-day-old seedlings were transferred 2 h in -Pi plates buffered at the indicated pH, containing 0 or 30 μM Al^{3+}. Bottom: representative pictures used for measurements.
Box plots indicate the median, the 25th to 75th percentiles (box edges) and the min to max range (whiskers); Mann-Whitney test; ****P<0.0001; **P<0.01; NS, not significant (P>0.05); number of nuclei per condition: a) 80-143; b) 102-125; c) 86-121). Bars, 100 μm.

Figure 6
ALS3 represses STOP1 accumulation in root nuclei.

WT and the *als3* mutant seedlings carrying the *pSTOP1::GFP-STOP1* construct were grown 3 days on a -Pi-Fe plate (made with agar Seakem), transferred to –Pi-Fe or –Pi + 60μM Fe plates for 2 h, and GFP-fluorescence was visualized by confocal microscopy. To avoid saturated GFP fluorescence in the images, the microscope was set on the highest fluorescence (as detected in *als3*). Bars = 100 μm.

Figure 7
Model depicting the roles of Fe and Al on the STOP1 signalling and root growth in relation with Pi availability.

Phosphate reversibly inactivates Fe and Al by forming a complex with them. Under -Pi condition and low-pH, Fe, Al or another unknown molecule accumulates in the cell where it decreases proteasomal degradation of STOP1 thereby stimulating the accumulation of STOP1 in the nucleus; nuclear STOP1 activates the transcription of *ALMT1*. The tonoplast-anchored ALS3 and STAR1 proteins pump the Fe, Al or the unknown molecule from the cytosol to the vacuole compartment, thereby decreasing its concentration in the cytosol. This reduces the accumulation of STOP1 in the nucleus and therefore the transcription of *ALMT1*. The ALMT1 transporter exudes malate in the apoplast where, together with Fe and the ferroxidase LPR1, they generate ROS that inhibit cell wall expansion. Exuded malate also chelates Al^{3+}, therefore preventing its toxicity (not shown in the scheme).

Red arrows: activation
Black arrow: proteasomal degradation
Blue blunt arrows: repression
Dashed arrows: transfer between compartments

Figure 1

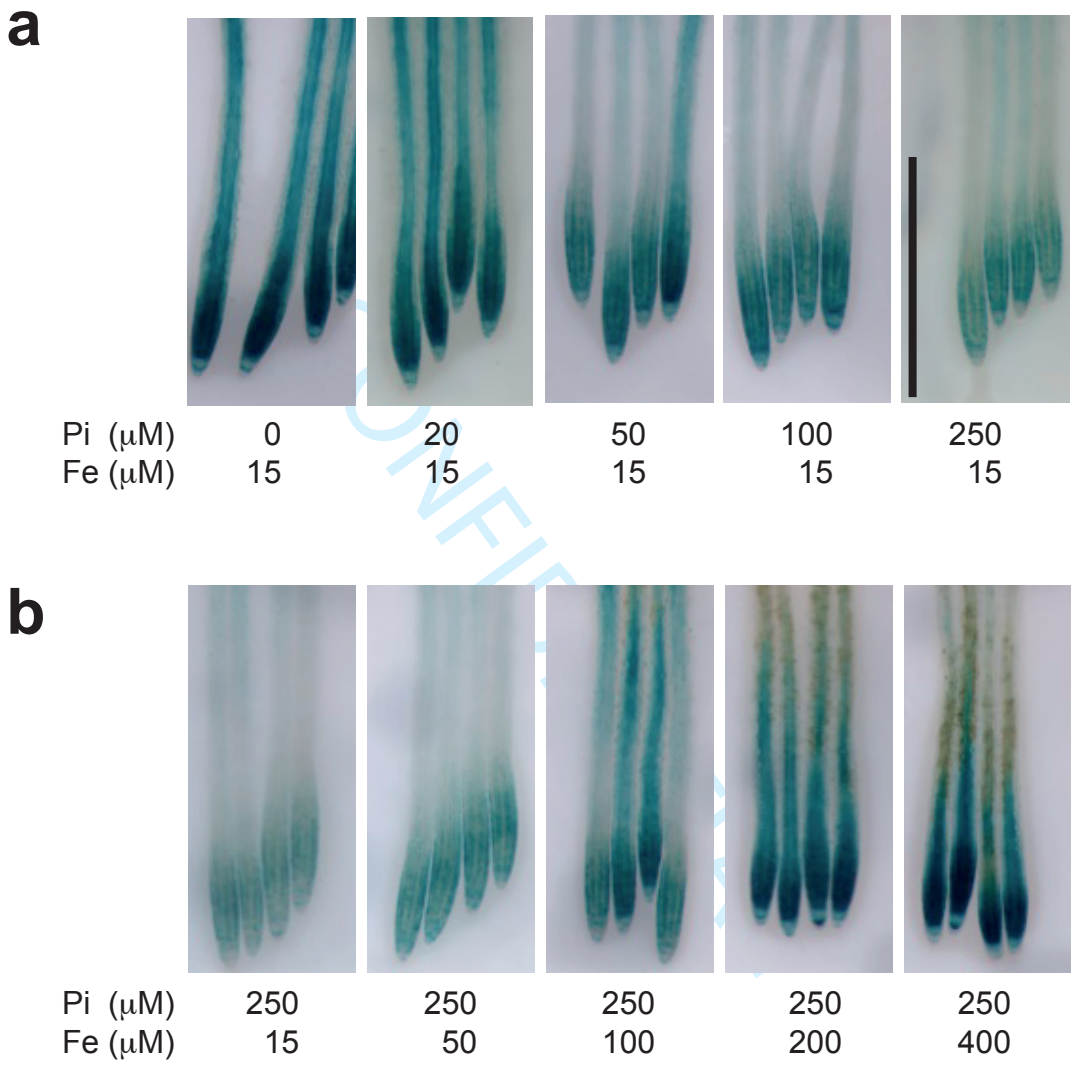
a
Pi (μM) 0 20 50 100 250
Fe (μM) 15 15 15 15 15
b
Pi (μM) 250 250 250 250 250
Fe (μM) 15 50 100 200 400

Figure 2

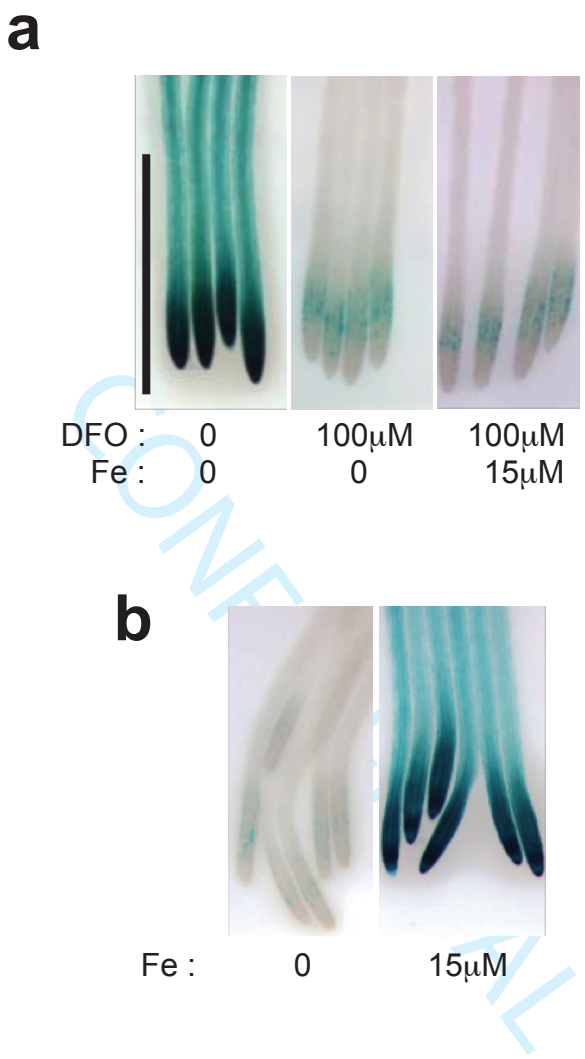

Figure 3

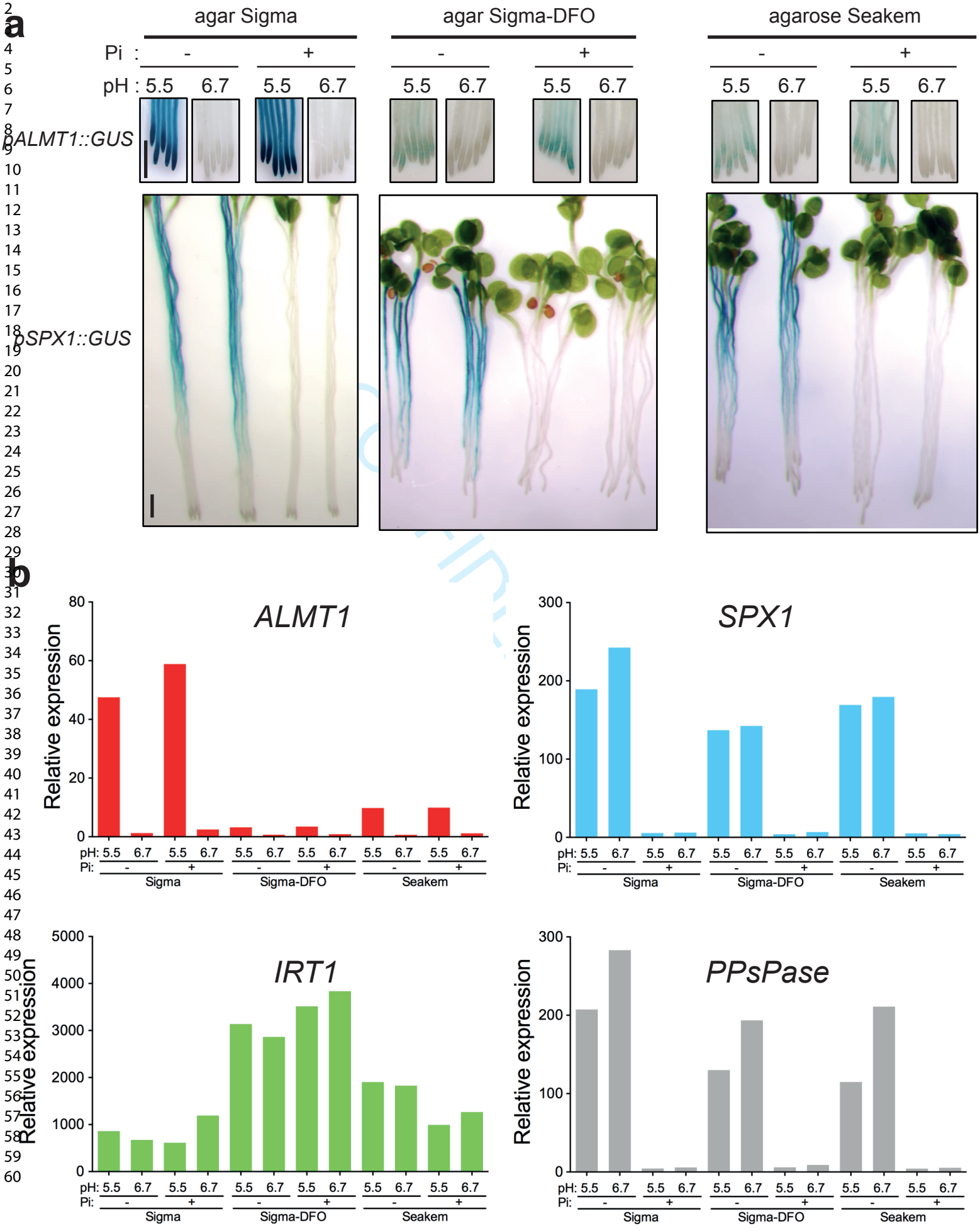
a
agar Sigma
agar Sigma-DFO
agarose Seakem
Pi : - + - + - +
pH : 5.5 6.7 5.5 6.7 5.5 6.7 5.5 6.7 5.5 6.7 5.5 6.7
pALMT1::GUS
pSPX1::GUS
b
ALMT1
SPX1
IRT1
PPsPase
Relative expression
pH: 5.5 6.7 5.5 6.7 5.5 6.7 5.5 6.7 5.5 6.7 5.5 6.7
Pi: - + - + - +
Sigma
Sigma-DFO
Seakem

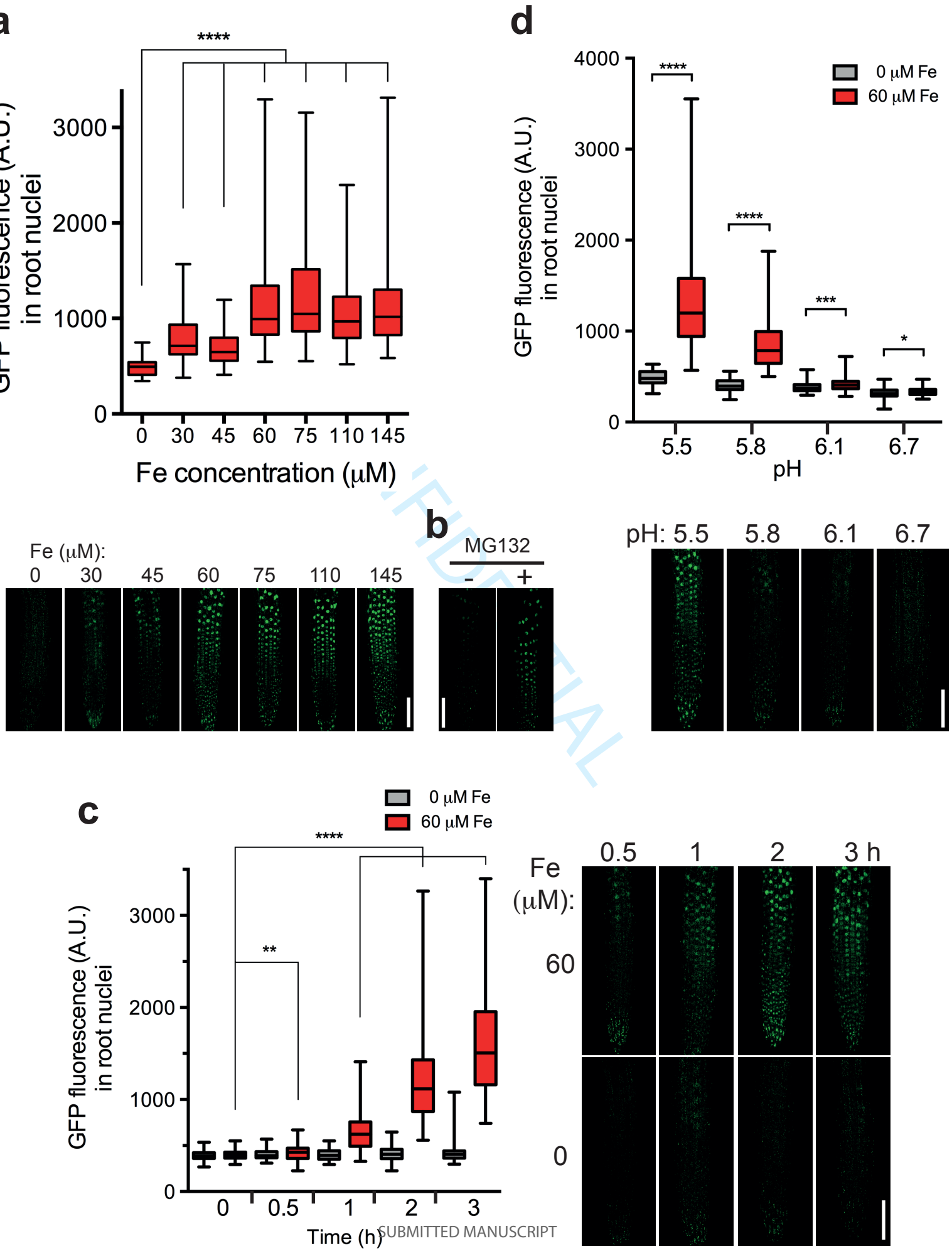

Figure 5

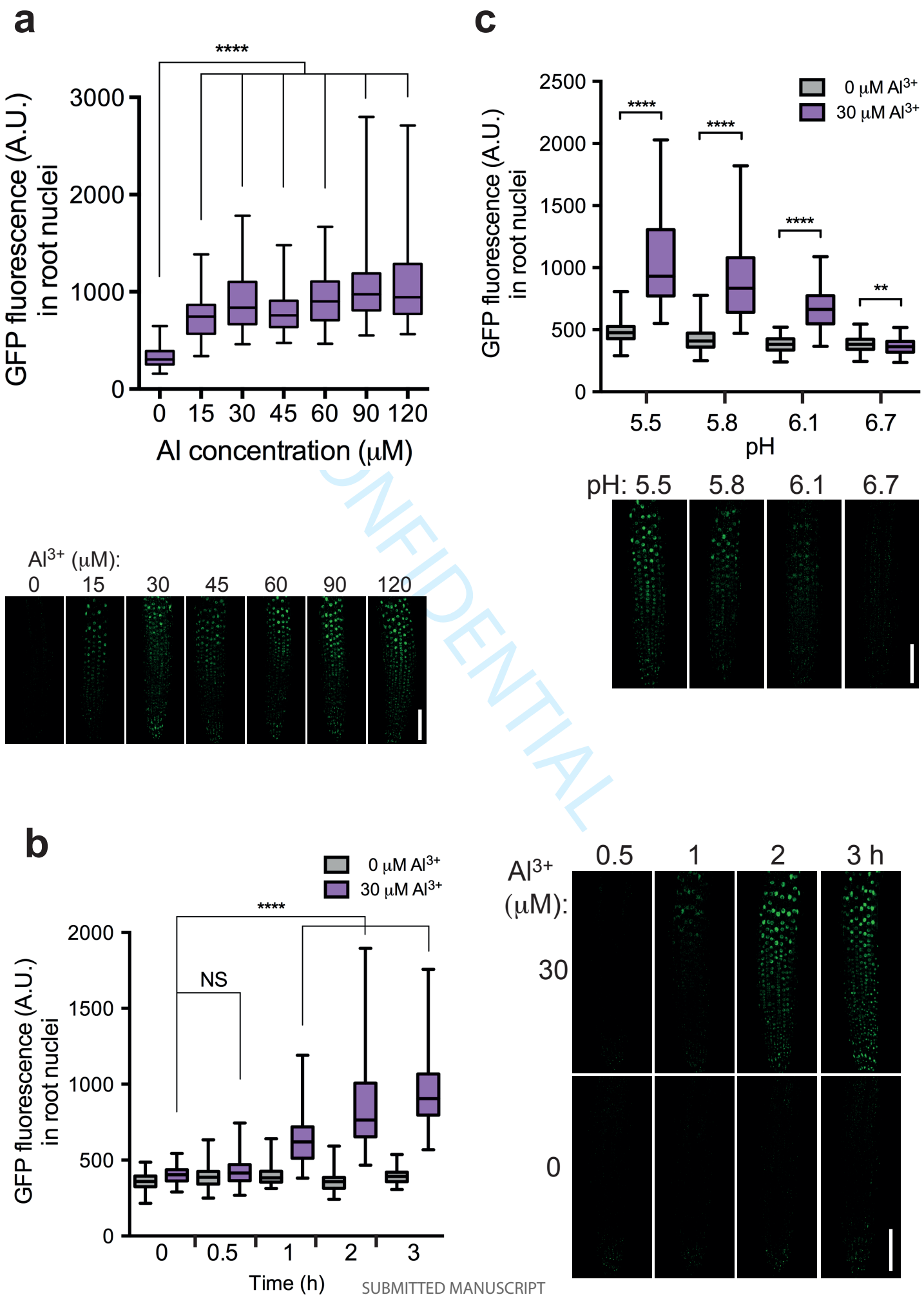

Figure 6

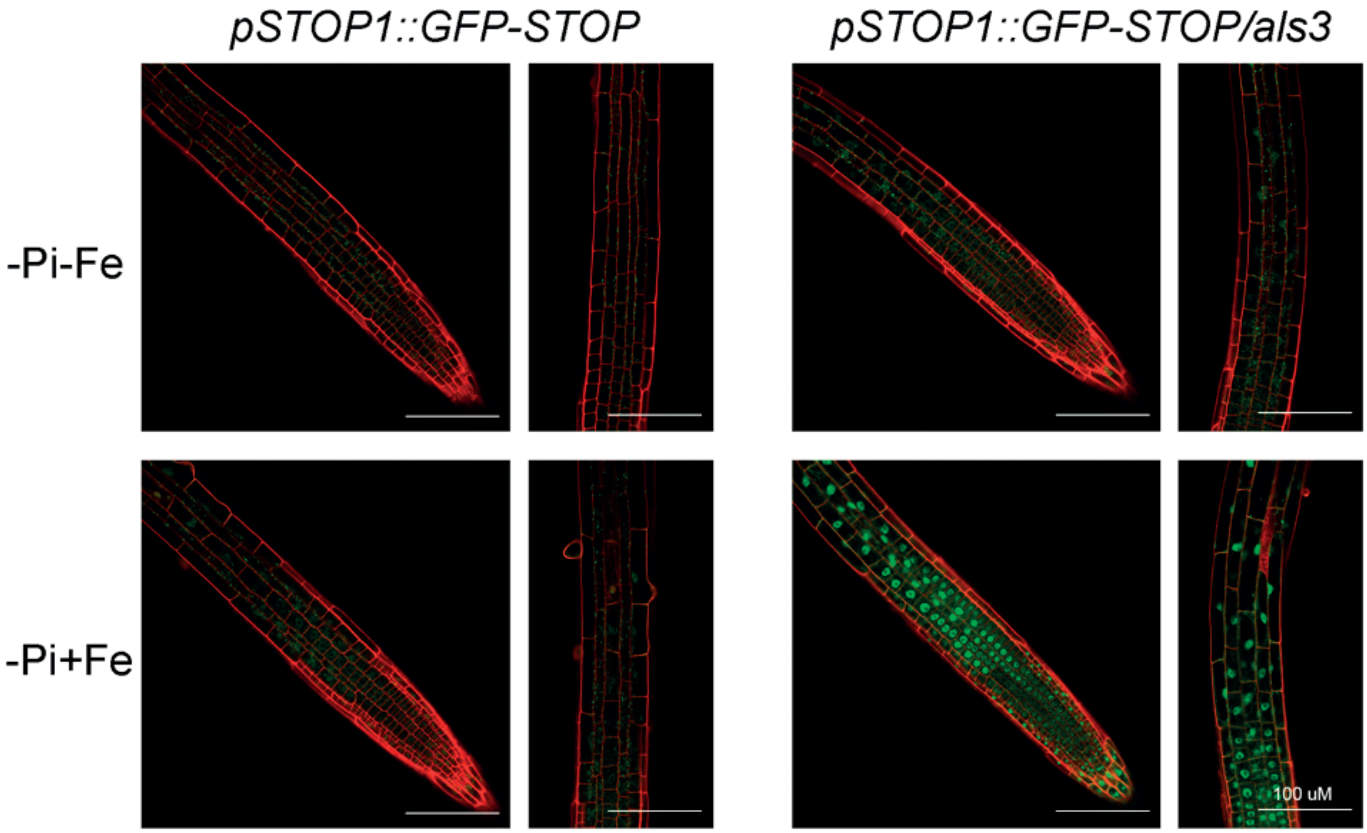

Figure 7

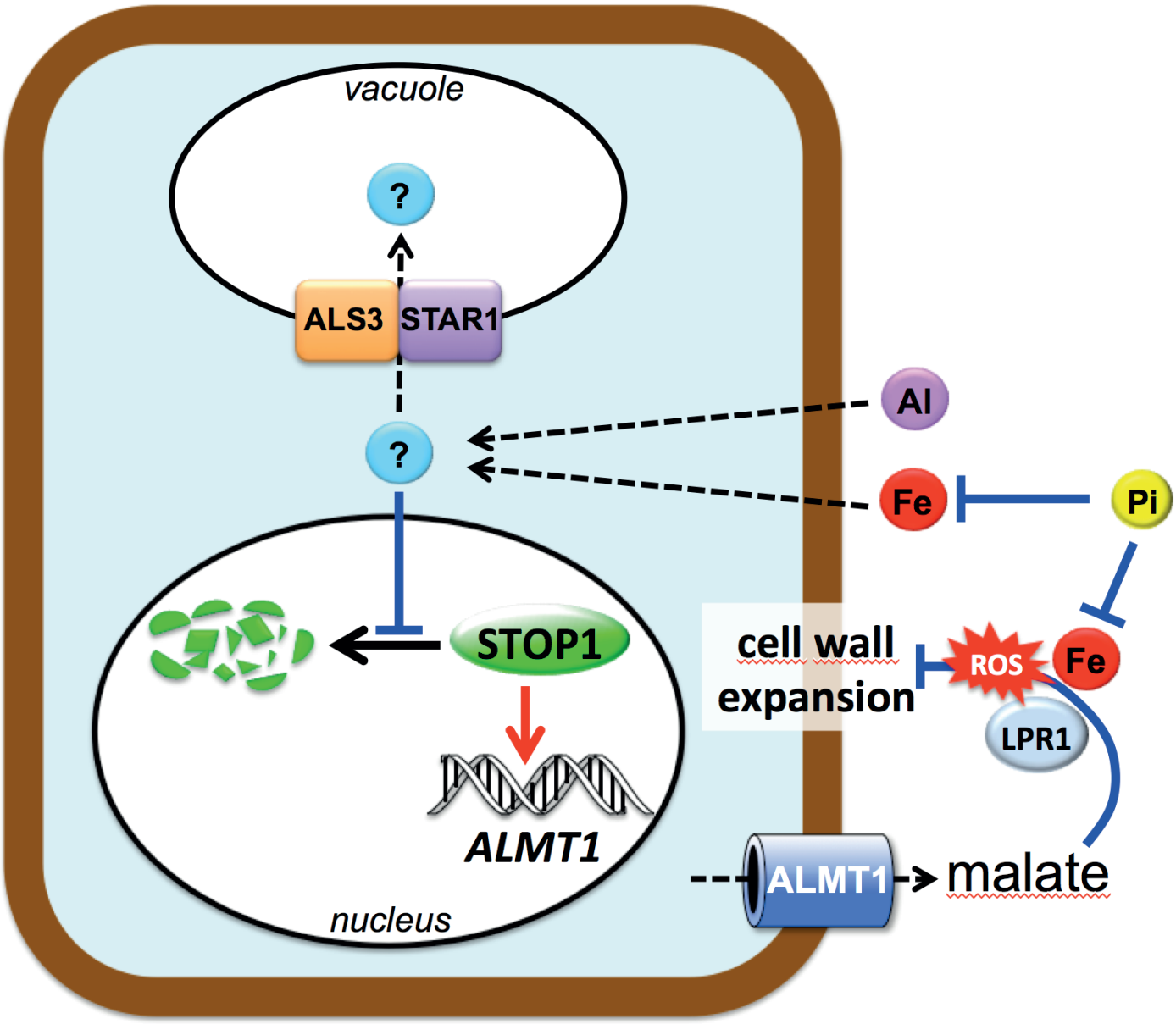
vacuole
?
ALS3
STAR1
Al
?
Fe
Pi
STOP1
cell wall
expansion
ROS
Fe
LPR1
ALMT1
ALMT1
malate
nucleus

Figure S1

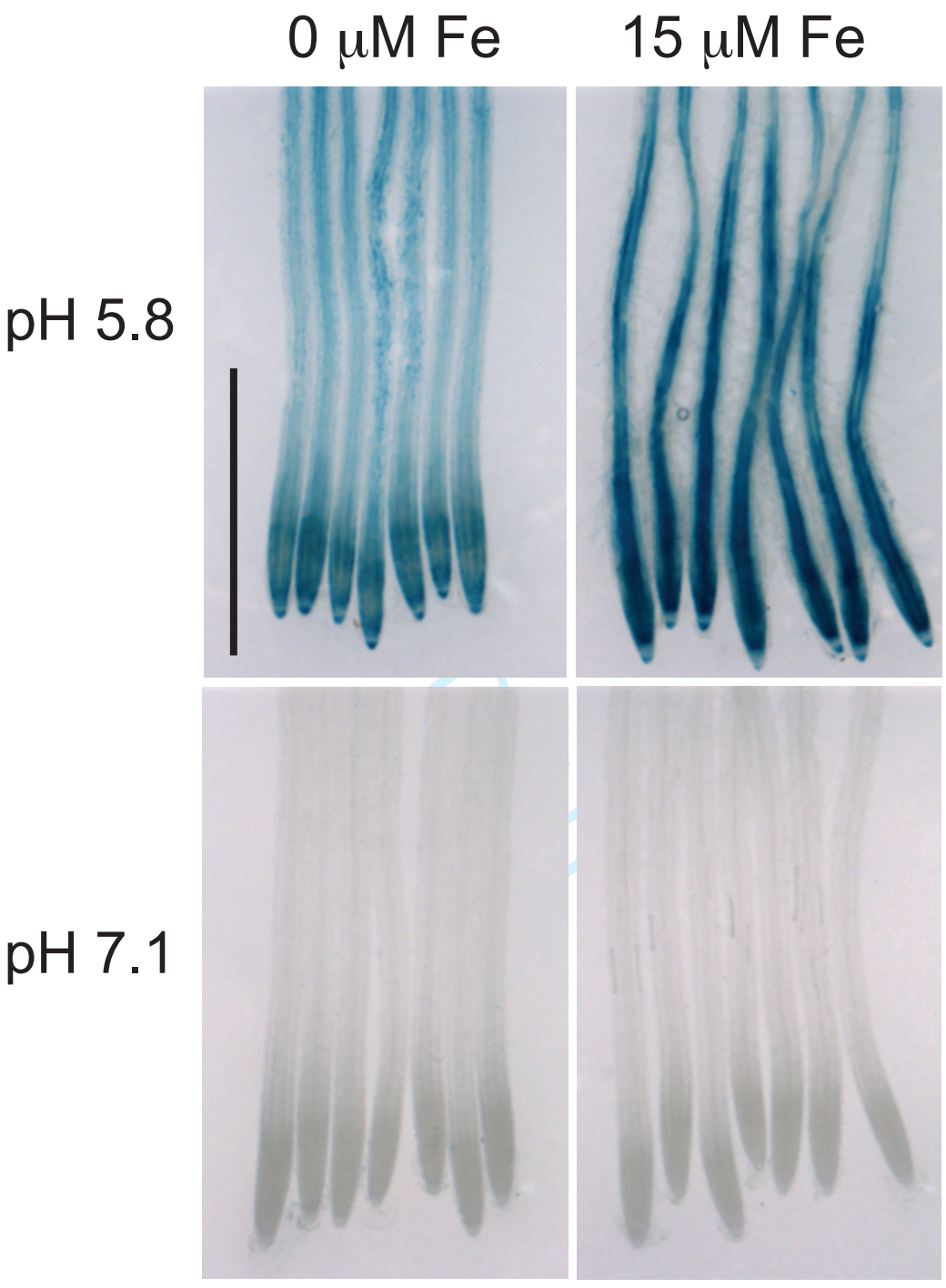

Figure S2

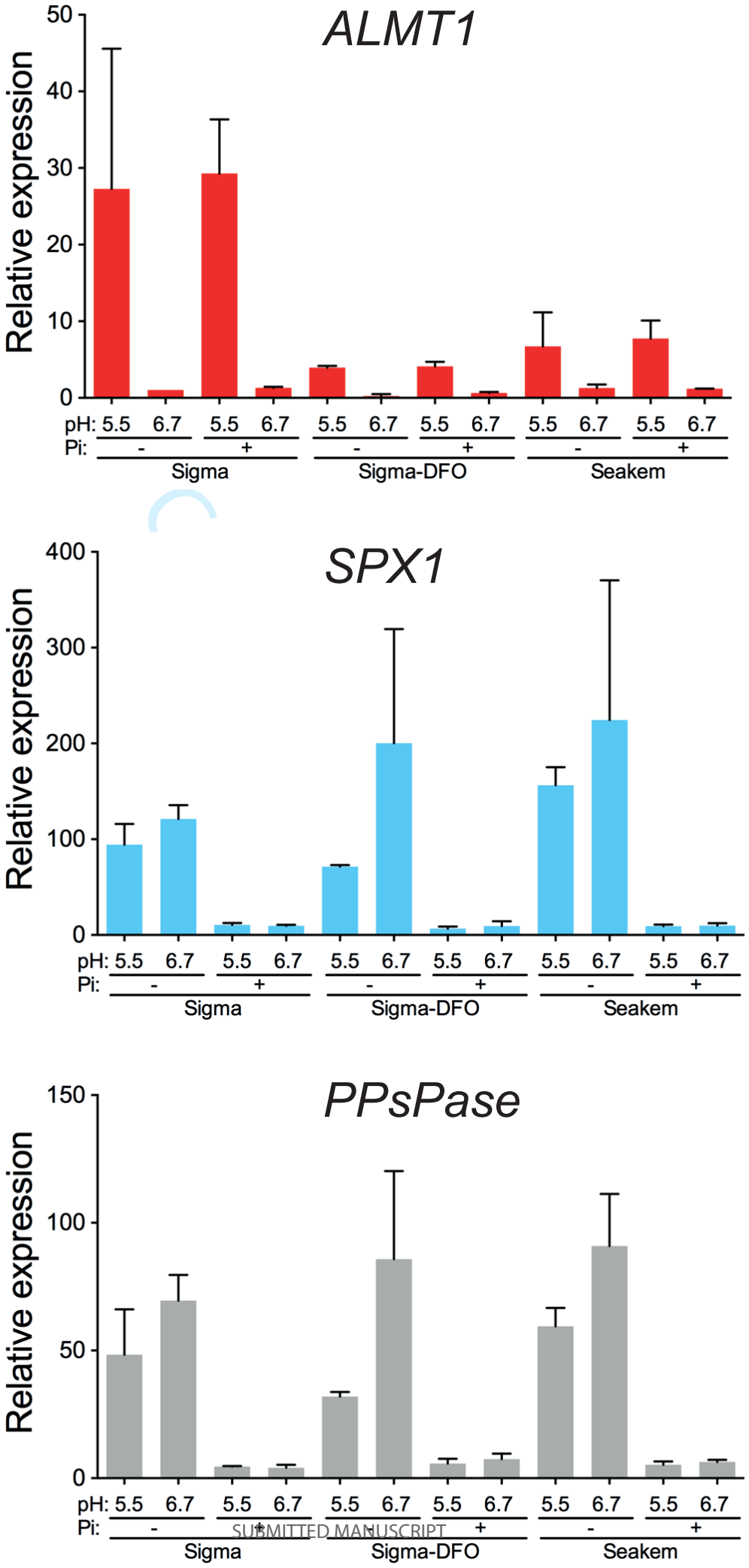

Figure S3

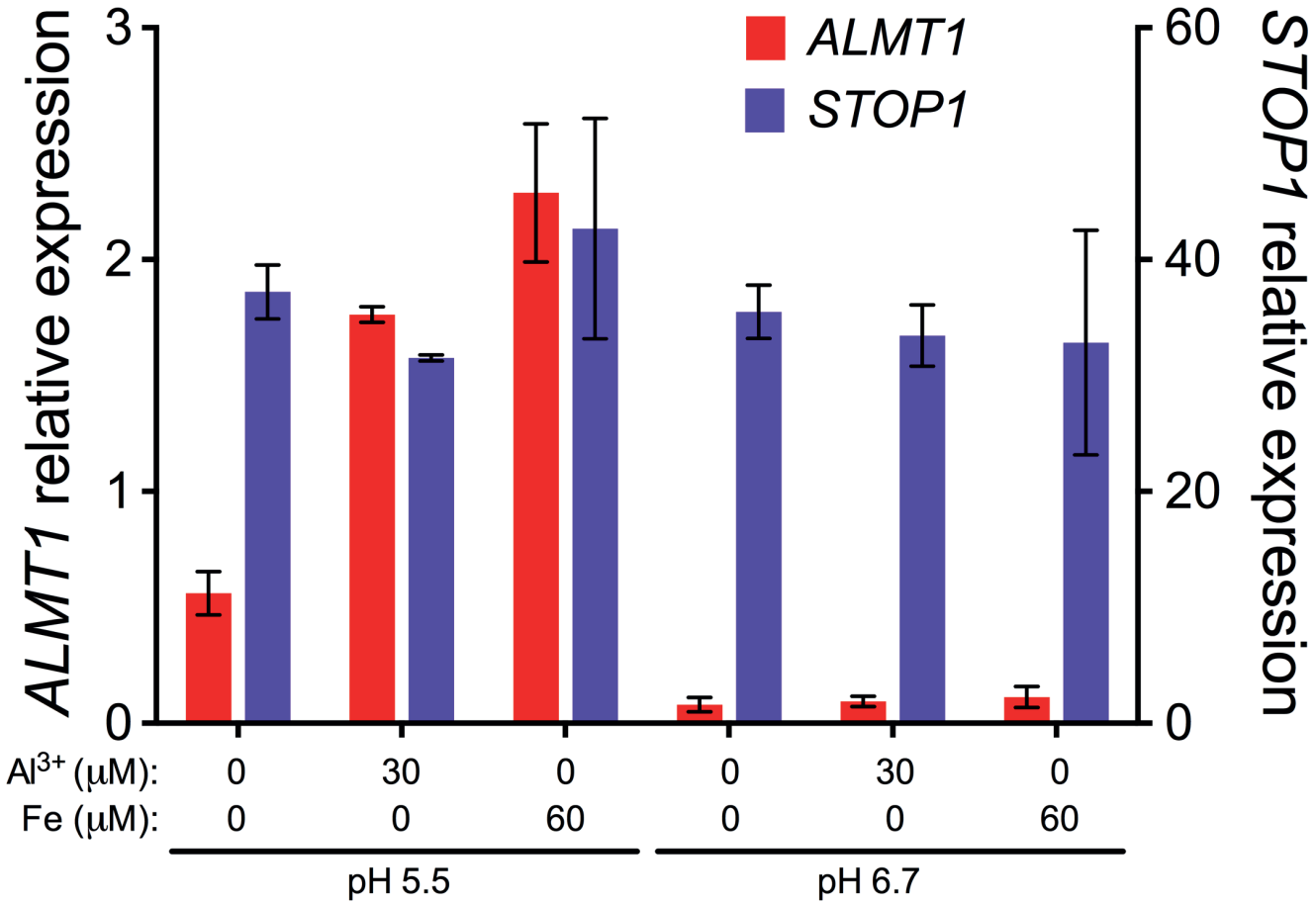
ALMT1 relative expression
STOP1 relative expression
ALMT1
STOP1
3
2
1
0
60
40
20
0
Al3+ (μM):
Fe (μM):
0
0
30
0
0
60
0
0
30
0
0
60
pH 5.5
pH 6.7

Figure S4

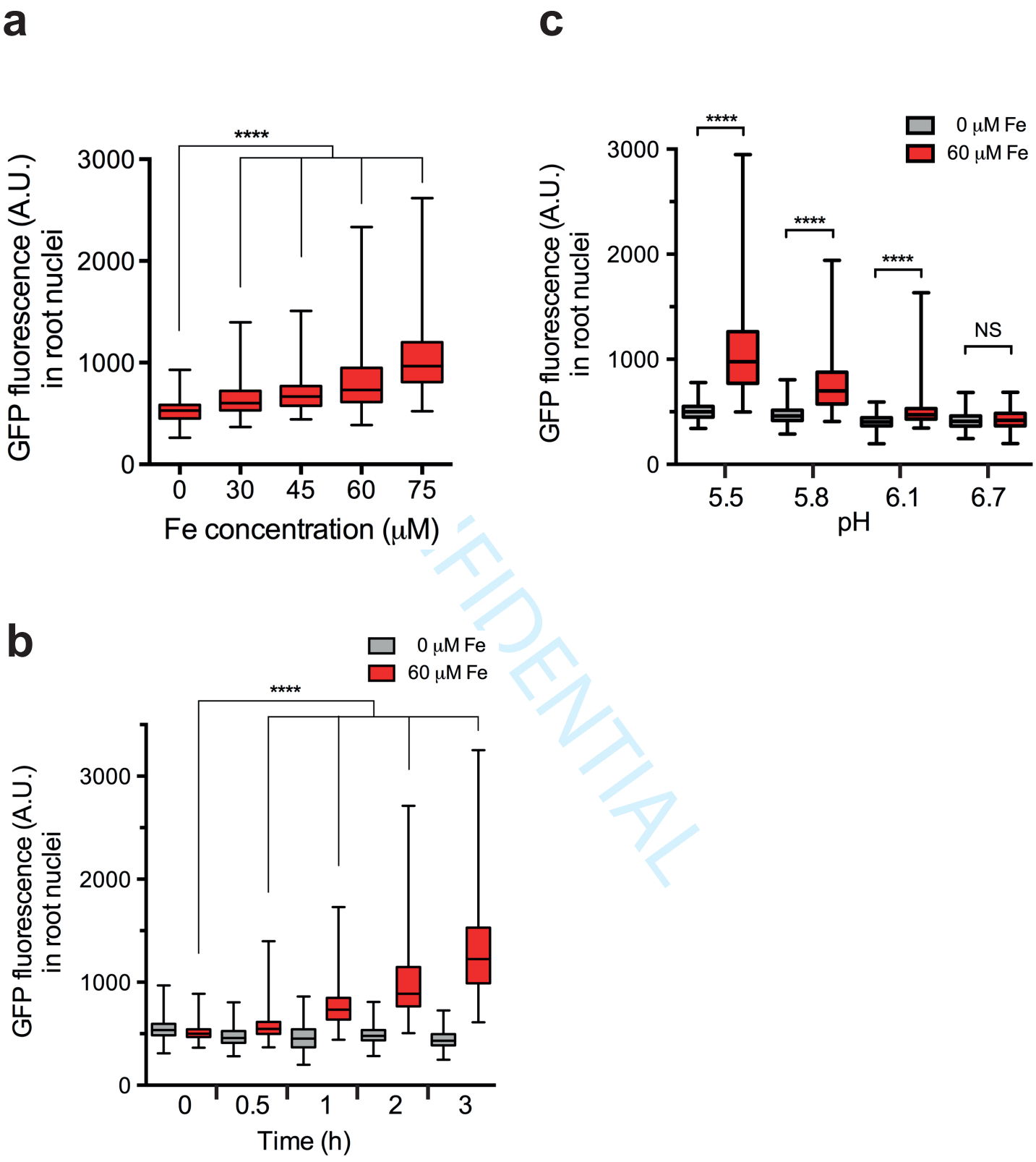

Figure S5

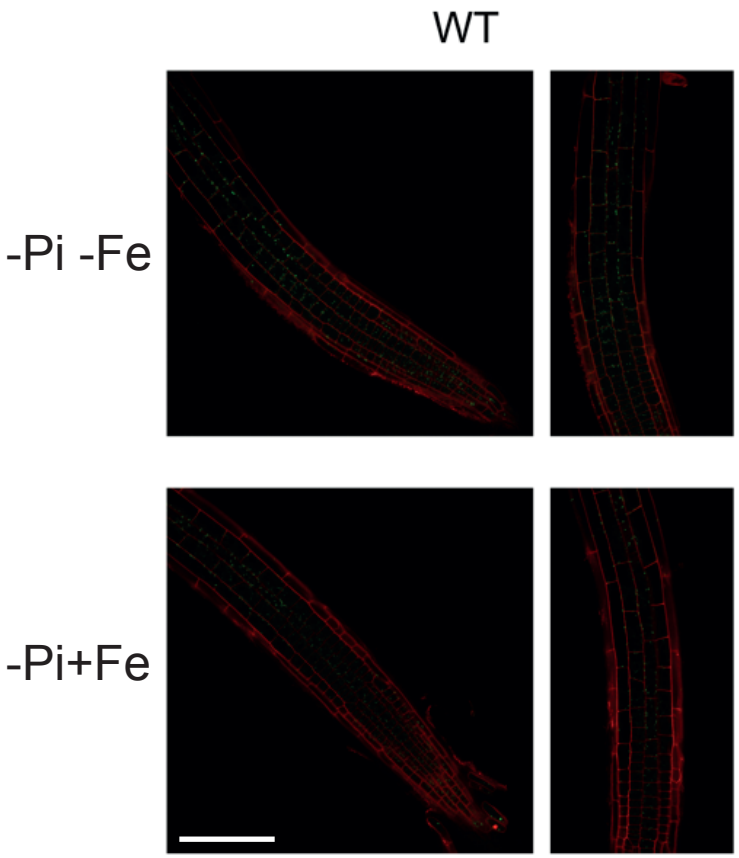

Figure S6

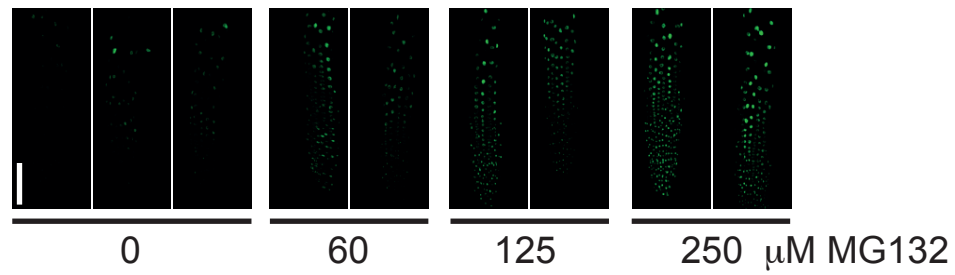

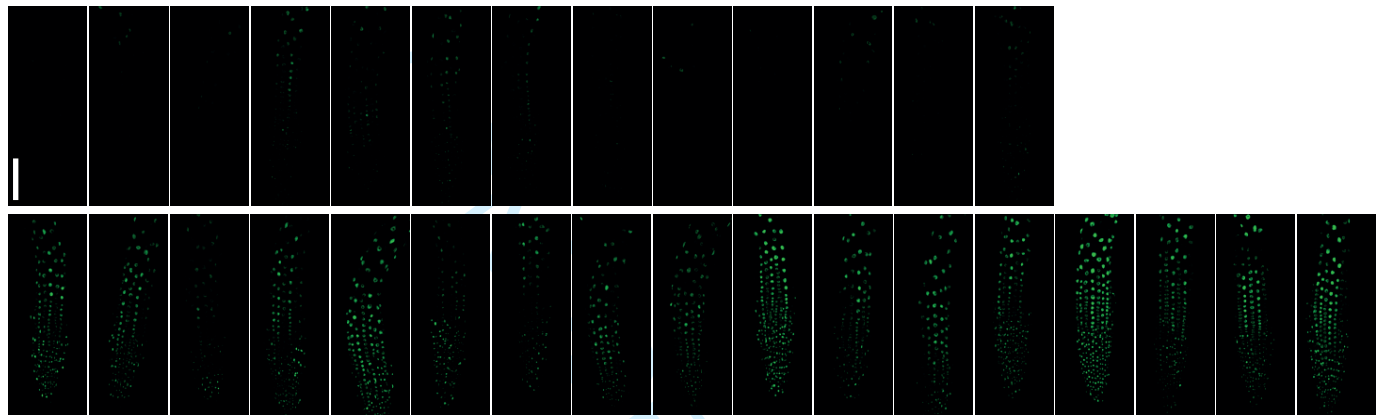

Figure S7

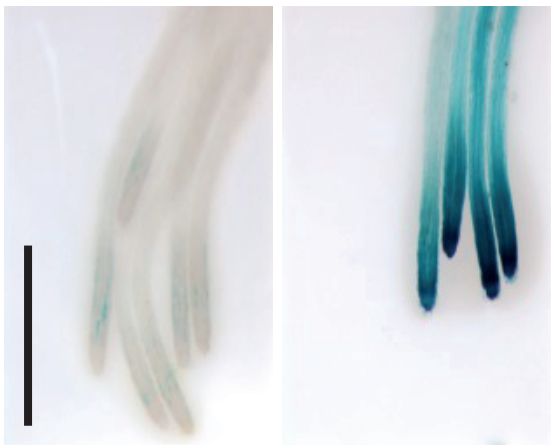

Figure S8

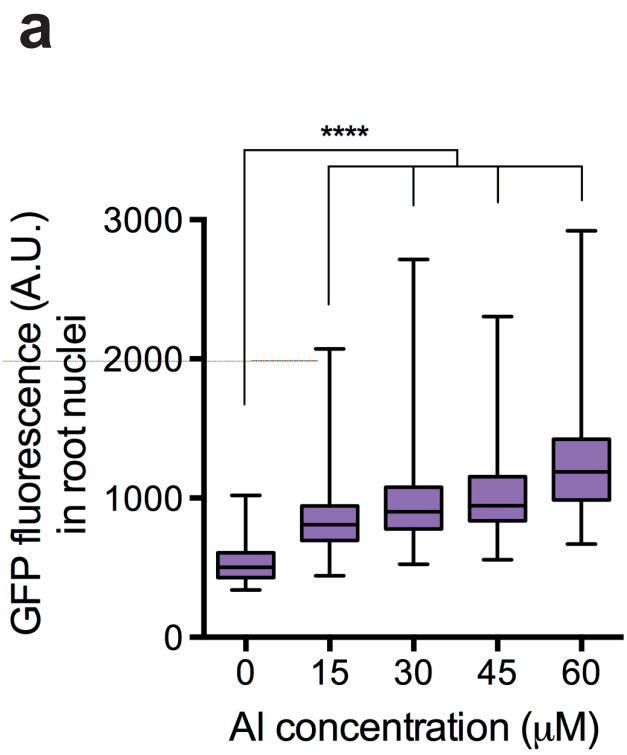

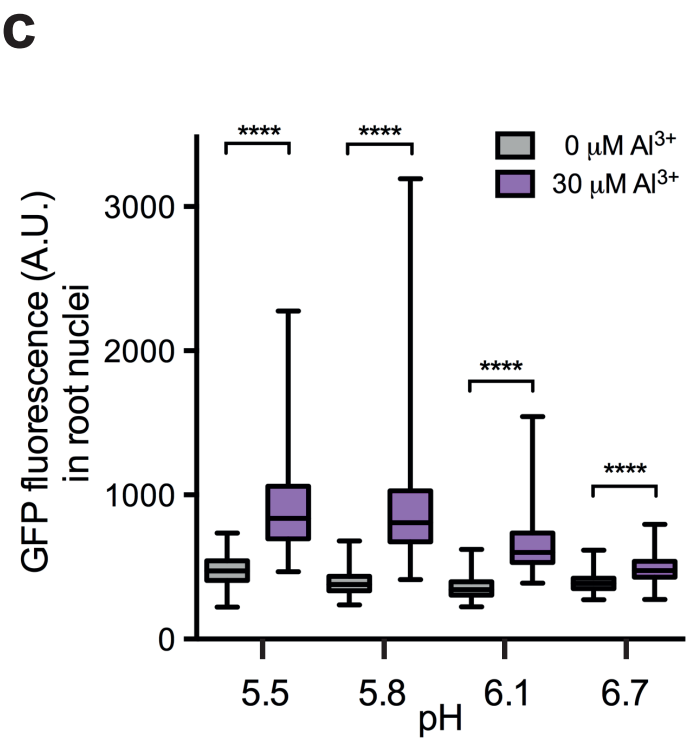

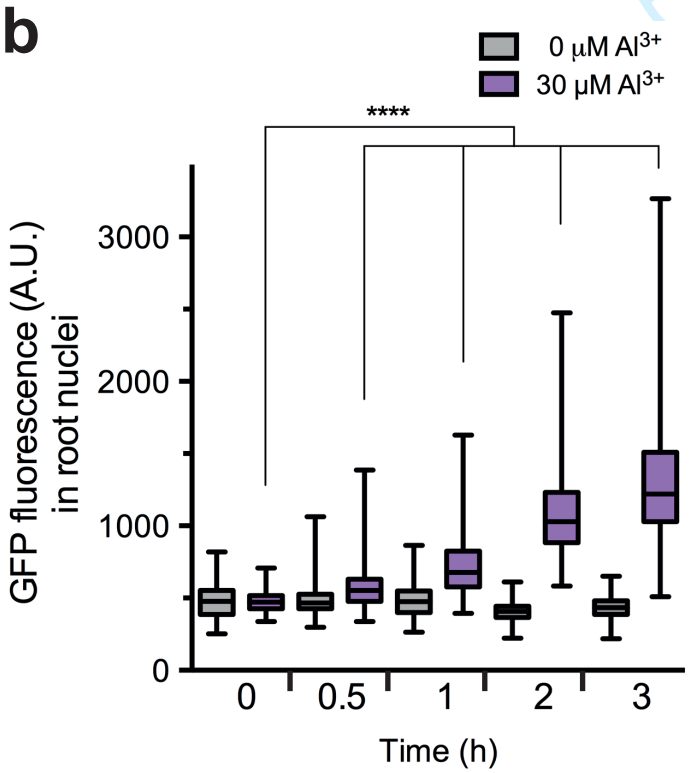

Figure S9